Mathematics

https://www.aimspress.com/journal/Math

AIMS Mathematics, 10(12): 30594–30622.
DOI: 10.3934/math.20251341
Received: 20 Ocrober 2025
Revised: 10 December 2025
Accepted: 16 December 2025
Published: 26 December 2025

Research article

Height–plane contact along edges, corners, and cusps

Fawaz Alharbi*

Department of Mathematics, Umm Al-Qura University, P.O.Box 21955, Postal Code 715, Makkah, Saudi Arabia

* **Correspondence:** Email: fdlohaibi@uqu.edu.sa.

Abstract: We study pairs $\widetilde{X} = (X, S)$ which consist of regular surfaces $X \subset \mathbb{R}^3$ endowed with a distinguished boundary S given by $y^2 - x^s = 0$ ($s = 1, 2, 3$: edge, corner, cusp). First, we give an explicit description of the logarithmic vector fields tangent to (g, b_s), $g = z - f(x, y)$. In particular, the five fields E, L, G_g, G_x, G_y generate $\mathrm{Der}(-\log(g, b_s))$. This yields a concrete Kodaira–Spencer calculus and a relative 2-determinacy theorem (with a single parabolic exception). Then, we classify submersions and obtain normal forms and mini versal unfoldings for submersion germs in codimension ≤ 2, with respect to the $\mathcal{R}(\widetilde{X})$-equivalence relation. Second, for height functions $h_v(w) = \langle w, v\rangle$ we obtain sharp linear conditions on $v \in S^2$ that characterize the A_k–contact along each boundary type. In particular, in the cuspidal case, the A_3/A_5 transition is governed by singular torsion. The resulting direction discriminant $\mathcal{D}_s \subset S^2$ corresponds, under the direction–parameter normalization, to a hyperplane arrangement of linear discriminant loci in the mini versal parameter spaces. Both the ambient discriminant $\mathfrak{D}_X$ and the boundary contact discriminants are invariant under P–$\mathcal{R}^+(\widetilde{X})$–equivalence.

Keywords: Bifurcation diagram; caustic; vector field; cuspidal edge; contact; curvatures and torsions; height function; deformations; discriminant
Mathematics Subject Classification: 57R45, 53A05

1. Introduction

In many applications and geometric aspects, regular surfaces X in $\mathbb{R}^3$ can have a distinguished curve S (smooth or singular). Such a configuration appears as a part of bifurcation diagrams and caustics of simple functions with respect to the quasi-equivalence relation which was discussed by Vladamir Zakalyukin in 2011 [1, 2]. This relation was later developed by the author and others to a more general setting, and the new relation was named the quasi-border equivalence relation [3, 4]. The bifurcation diagrams of Morse functions under this new equivalence relation exhibit regular surfaces endowed with boundary curves of types $s = 1, 2, 3$ (smooth edge, corner, cusp) [4, 5]. Some authors have recently begun to address these phenomena, including genericity of caustics and wavefronts on an r-corner [6], the study of vector fields on bifurcation diagrams and caustics with respect to quasi equivalences [7] and height functions on a singular surface with a distinguished curve [8]. From a geometric side, the theory of fronts provides a coherent framework, with detailed invariants for cuspidal edges and their folded variants [9–11], while logarithmic derivations and discriminants of divisors and arrangements offer a complementary algebraic perspective [12–14]. In addition, recent studies in *AIMS Mathematics* on framed/frontals and singular surfaces provide context for the present work [15–17].

We adopt a relative point of view similar to a quasi–equivalence case: fix a surface with boundary $\widetilde{X} = (X, S)$, where locally X is in Monge form, and S is one of the standard germs $b_s = y^2 - x^s = 0$, $s = 1, 2, 3$ (smooth edge, corner, cusp). Throughout, mappings and vector fields are required to preserve $\widetilde{X}$. For submersion germs $h : (\mathbb{R}^3, 0) \to (\mathbb{R}, 0)$ under $\mathcal{R}(\widetilde{X})$-equivalence relation, we introduce a restricted Kodaira–Spencer map on 1– and 2–jets, prove a relative 2–determinacy theorem, and list normal forms and mini versal unfoldings in codimension ≤ 2. The jet level image precisely records the missing linear or quadratic terms and hence the unfolding parameters.

A central goal of the paper is to study the contact of height planes with curves on a regular surface. For a unit vector $v \in S^2$, if we restrict the ambient height $h_v(w) = \langle w, v \rangle$ to X and then to the distinguished curve γ_s, we obtain a one variable germ whose order of vanishing detects A_k–contact. We give sharp criteria, for each $s = 1, 2, 3$, and show how simple linear conditions on v force contact jumps $A_0 \to A_1 \to A_2 \to \cdots$.

The present work differs from earlier studies such as [9–11] in several essential ways. Those papers focus on the intrinsic or extrinsic geometry of singular surfaces including cuspidal edges, folded cuspidal edges, focal surfaces of parabolic points, and the theory of fronts, and provide geometric invariants and classifications within those settings. In contrast, our point of view is relative: we fix a regular surface X together with a distinguished boundary S of one of the types $s = 1, 2, 3$ and study submersion germs and height functions up to the restricted $\mathcal{R}(\widetilde{X})$–equivalence, preserving this pair. This requires establishing a logarithmic tangent module $\mathrm{Der}(-\log(g, b_s))$, developing a restricted Kodaira–Spencer calculus, and proving a relative 2–determinacy theorem. These tools allow us to classify all submersion germs of codimension ≤ 2 on (X, S) and to give explicit A_k–criteria for height–plane contact along each boundary type. Furthermore, the resulting direction discriminants correspond to linear hyperplane arrangements in the miniversal parameter spaces, a phenomenon not addressed in the aforementioned works.

In summary, the main contributions of this paper are as follows:

(1) We introduce a logarithmic tangent module $\mathrm{Der}(-\log(g, b_s))$ adapted to a regular surface with a distinguished boundary and develop a restricted Kodaira–Spencer calculus for this setting.

(2) We establish a relative 2–determinacy theorem and use it to classify all submersion germs on (X, S) of codimension ≤ 2 under the restricted $\mathcal{R}(\widetilde{X})$–equivalence.

(3) For height functions h_v, we obtain explicit linear conditions on the viewing direction $v \in S^2$ characterizing the boundary contact types A_k for each of the three boundary models $s = 1, 2, 3$.

(4) We show that the corresponding direction discriminants on S^2 pull back from linear hyperplane arrangements in the miniversal unfolding spaces and that these discriminants are invariant under P–$\mathcal{R}^+(\widetilde{X})$–equivalence.

For accessibility, we briefly list the principal results proved in the paper:

(1) Theorem 2.18 establishes a relative 2–determinacy theorem for submersion germs on (X, S) with respect to the restricted $\mathcal{R}(\widetilde{X})$–equivalence.

(2) Theorem 2.21 gives a complete classification of all submersion germs with $\mathcal{R}(\widetilde{X})$–codimension ≤ 2; together with their miniversal unfoldings, distinguishing the elliptic/hyperbolic and parabolic cases.

(3) Propositions 3.1–3.3 provide explicit A_k–contact criteria for the height function along the boundary curves γ_1, $\gamma_{2,\pm}$, and γ_3, expressed as sharp linear conditions on the viewing direction $v \in S^2$.

(4) Corollary 4.4 describes the direction discriminants $\mathcal{D}_s \subset S^2$ and shows that they correspond, under the direction–parameter normalization, to hyperplane arrangements in the associated miniversal parameter spaces.

The paper is organized as follows. In Section 2, we set up models $\widetilde{X}_0 = (X_0, S_0)$ for normal forms of regular surfaces

$$X_0 = \{g = z - f^*(x, y) = 0\} \subset \mathbb{R}^3, f^*(x, y) \in \{\, x^2 + y^2 \text{ (elliptic)},\ x^2 - y^2 \text{ (hyperbolic)},\ x^2,\ y^2 \text{ (parabolic)}\,\};$$

with distinguished curves $S_0 = \{b_s = g = 0\} \subset X_0$, $s \in \{1, 2, 3\}$ (smooth edge, corner, cusp) and then describe the generators of $\mathrm{Der}(-\log(g, b_s))$, which preserve such models $\widetilde{X}_0$. We then construct the restricted Kodaira–Spencer map, establish relative 2–determinacy with respect to an $\mathcal{R}(\widetilde{X})$-equivalence relation which keeps $\widetilde{X}_0$ fixed in line with the quasi-equivalence setting. After that, we give the codimension ≤ 2 classification of submersions on $\widetilde{X}_0$ with mini–versal unfoldings. In Section 3.1, we discuss the height functions in $\widetilde{X}_0$ and derive A_k criteria along the three types of boundaries. In addition, we discuss the identification of the linear direction discriminant on S^2 with the linear arrangement of strata in the mini versal parameter spaces.

2. A regular surface with a distinguished boundary curve

Let X be a regular surface in $\mathbb{R}^3$ at the origin. So, we may assume that X is the graph of a function $z = f(x, y)$ with $f(0, 0) = 0$ and $\nabla f(0, 0) = 0$. Thus,

$$\Gamma : U \subset \mathbb{R}^2 \longrightarrow \mathbb{R}^3, \qquad (x, y) \longmapsto (x, y, f(x, y))$$

is a local parameterization of X in an open neighborhood U of $(0, 0)$, where

$$f(x, y) = \tfrac{1}{2}\Big(k_1 x^2 + k_2 y^2\Big) + a_{30}x^3 + a_{21}x^2 y + a_{12}xy^2 + a_{03}y^3 + O(\|(x, y)\|^4),$$

with k_1, k_2 as the principal curvatures of X at 0.

Fix an integer $s \geq 1$ and define a *distinguished boundary curve* as

$$S = \{(x, y, f(x, y)) \in X :\ y^2 - x^s = 0\} = \Gamma(\{(x, y) \in \mathbb{R}^2 :\ y^2 - x^s = 0\}).$$

We refer to $\widetilde{X} = (X, S)$ as a regular surface endowed with a distinguished boundary curve. For $s = 1, 2, 3$, the plane curve $y^2 - x^s = 0$ is a smooth branch, two transversely intersecting branches (a corner), and an ordinary cusp, respectively.

Because $\nabla f(0,0) = 0$, the tangent cone to X at 0 is $T_0X = \{z = 0\}$. Moreover, the tangent cone of S lies inside $\{z = 0\}$ and depends on s as detailed below.

• **For** $s = 1$ **(smooth boundary).** The curve S has the parameterization

$$\gamma_1(t) = (t^2,\ t,\ f(t^2, t)).$$

Then $\gamma_1'(0) = (0, 1, 0)$, which implies that the tangent cone of S is the single line

$$\{x = 0,\ z = 0\} \subset \{z = 0\},$$

directed along the y-axis.

Proposition 2.1. *(1) A normal vector to the osculating plane of S at 0 is $(-\frac{k_2}{2},\ 0,\ 1)$ (up to a nonzero scalar multiple).*

(2) The osculating plane has equation

$$k_2\, x - 2z = 0.$$

Proof. If we differentiate $\gamma_1(t)$ twice, we obtain $\gamma_1''(0) = (2, 0, k_2)$. Hence, $\gamma_1'(0) \times \gamma_1''(0) = (k_2, 0, -2)$, which is proportional to $(-\frac{k_2}{2}, 0, 1)$. Therefore, the plane with this normal is $k_2 x - 2z = 0$. □

• **For** $s = 2$ **(corner).** The curve $S = \{y^2 - x^2 = 0\}$ consists of two smooth branches with parameterizations.

$$\gamma_{2,+}(t) = (t,\ t,\ f(t, t)), \qquad \gamma_{2,-}(t) = (t,\ -t,\ f(t, -t)).$$

Then $\gamma_{2,+}'(0) = (1, 1, 0)$ and $\gamma_{2,-}'(0) = (1, -1, 0)$. Thus, the tangent cone of S is the union of the two distinct lines in $\{z = 0\}$ along $y = \pm x$. Let

$$u_\pm = \frac{1}{\sqrt{2}}(1, \pm 1)$$

be the unit tangent directions of the branches in the xy-plane.

Proposition 2.2. *The normal curvature of X in 0 along both directions of the branch is*

$$k_n(u_+) = k_n(u_-) = \tfrac{1}{2}\,(k_1 + k_2).$$

Proof. Let θ be the angle between the tangent direction and the x-axis. Then, the respective Euler formula is $k_n(\theta) = k_1 \cos^2\theta + k_2 \sin^2\theta$. For $u_\pm$, we have $\theta = \pm\frac{\pi}{4}$. This implies that $\cos^2\theta = \sin^2\theta = \frac{1}{2}$. Thus,

$$k_n(u_\pm) = H(0) = \tfrac{1}{2}(k_1 + k_2).$$

□

• **For** $s = 3$ **(cusp).** Here $S = \{y^2 - x^3 = 0\}$ has parameterization

$$\gamma_3(t) = (t^2,\ t^3,\ f(t^2, t^3)).$$

We have $\gamma_3'(0) = (0, 0, 0)$ and $\gamma_3''(0) = (2, 0, 0)$. Hence, the tangent cone of S is the line $\{y = 0,\ z = 0\} \subset \{z = 0\}$.

Following [10], a singular space curve γ with $\gamma'(0) = 0$ is of *A-type* if $\gamma''(0) \neq 0$. Moreover, it is of $(2, 3)$-*type* if $\gamma''(0) \times \gamma'''(0) \neq 0$. The cuspidal curvature and singular torsion at 0 are defined by

$$\kappa_{\text{sing}}(\gamma, 0) = \frac{\left\|\gamma''(0) \times \gamma'''(0)\right\|}{\|\gamma''(0)\|^{5/2}}, \qquad \tau_{\text{sing}}(\gamma, 0) = \frac{\sqrt{\|\gamma''(0)\|}\ \det(\gamma''(0), \gamma'''(0), \gamma^{(4)}(0))}{\left\|\gamma''(0) \times \gamma'''(0)\right\|^2}.$$

Proposition 2.3. *The curve* γ_3 *is of* $(2, 3)$-*type at* 0. *Moreover,*

$$\kappa_{\text{sing}}(\gamma_3, 0) = \frac{3}{\sqrt{2}}, \qquad \tau_{\text{sing}}(\gamma_3, 0) = \sqrt{2}\, k_1.$$

In particular, $\kappa_{\text{sing}}'(\gamma_3, 0) = 0$.

Proof. We have $\gamma_3''(0) = (2, 0, 0)$ and $\gamma_3'''(0) = (0, 6, 0)$. Also, we have $\gamma_3''(0) \times \gamma_3'''(0) = (0, 0, 12) \neq 0$. This means that it is $(2, 3)$-type. Note that, $\gamma_3^{(4)}(0) = (0, 0, 12k_1)$. Hence,

$$\kappa_{\text{sing}}(\gamma_3, 0) = \frac{12}{2^{5/2}} = \frac{3}{\sqrt{2}}, \qquad \tau_{\text{sing}}(\gamma_3, 0) = \frac{\sqrt{2} \cdot (2 \cdot 6 \cdot 12k_1)}{12^2} = \sqrt{2}\, k_1.$$

On the other hand,

$$\kappa_{\text{sing}}(\gamma_3, t) = \frac{3}{\sqrt{2}} + \frac{3}{\sqrt{2}}\Big(2k_1^2 - \frac{45}{4}\Big)t^2 + O(t^4),$$

which implies that $\kappa_{\text{sing}}'(\gamma_3, 0) = 0$, as claimed. □

The preceding discussion is summarized in Table 1.

Table 1. Tangent cone of S.

s	boundary type	tangent cone of S in $z = 0$	directions in xy-plane
1	smooth boundary	single line along y-axis	$(0, 1)$
2	corner	two lines along $y = \pm x$	$(1, 1)$ and $(1, -1)$
3	cusp	single line along x-axis	$(1, 0)$

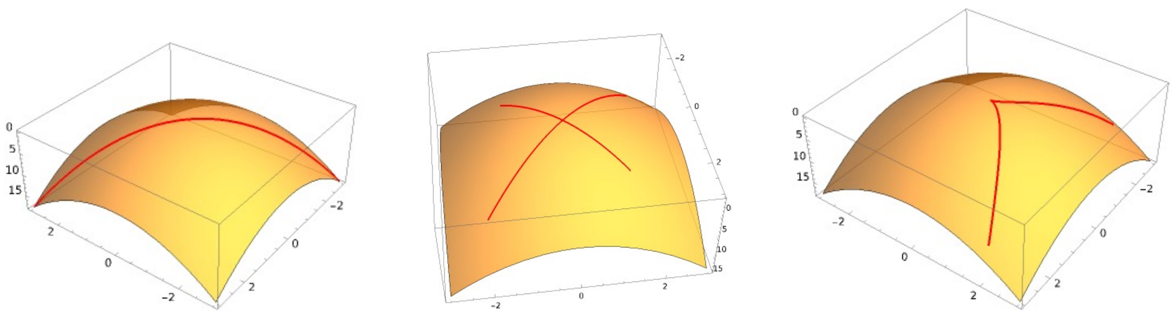

(a) Smooth boundary **(b)** Corner **(c)** Cusp

Figure 1. A regular surface with a distinguished boundary curve.

We now introduce function germs on a regular surface with a distinguished boundary. Then, we define the equivalence relations and tangent modules that govern their classification.

Let $U \subset \mathbb{R}^2$ be an open neighborhood of the origin. We consider the surface germ in Monge form

$$\widetilde{\Gamma}\colon (U,0) \longrightarrow (\mathbb{R}^3,0), \qquad (x,y) \longmapsto (x,\ y,\ f^*(x,y)).$$

Here f^* denotes one of the quadratic normal forms up to $\mathcal{A}$–equivalence (changes of local coordinates in source and target) [25, Chap. 11, pp. 251-252], namely

$$f^*(x,y) \in \{\, x^2+y^2 \text{ (elliptic)},\ x^2-y^2 \text{ (hyperbolic)},\ x^2,\ y^2 \text{ (parabolic)}\,\}.$$

Fix one of the three plane–curve germs at the origin

$$b_1(x,y) = y^2 - x, \qquad b_2(x,y) = y^2 - x^2, \qquad b_3(x,y) = y^2 - x^3,$$

and write

$$\beta_s := V(b_s) \subset (\mathbb{R}^2,0), \qquad s \in \{1,2,3\},$$

where $V(b_s)$ is the zero locus of b_s.

Set

$$X_0 := \widetilde{\Gamma}(U) \subset (\mathbb{R}^3,0), \qquad S_0 := \widetilde{\Gamma}(\beta_s) \subset X_0.$$

Definition 2.4. *We call the pair of germs*

$$\widetilde{X}_0 = (X_0, S_0) = (\widetilde{\Gamma}(U),\, \widetilde{\Gamma}(\beta_s))$$

a model of a regular surface with a distinguished boundary of type s.

Remark 2.5. *The twelve combinations of (f^*, β_s) (four quadratic point types $\times$ three boundary types) are the model pairs used below to analyze function germs on (X,S). Also, these are used to compute modules of vector fields tangent to the surface with a distinguished boundary.*

Denote by $\mathcal{E}_3$ (also $\mathcal{E}_w$ with $w = (x,y,z)$) the $\mathbb{R}$–algebra of smooth function germs $(\mathbb{R}^3,0) \to \mathbb{R}$. Also, denote by $\mathcal{M}_3$ its maximal ideal, and by θ_3 the $\mathcal{E}_3$–module of vector field germs on $(\mathbb{R}^3,0)$.

Definition 2.6. *A diffeomorphism germ $\varphi : (\mathbb{R}^3,0) \to (\mathbb{R}^3,0)$ is said to preserve $\widetilde{X}_0$ if*

$$\varphi(X_0) = X_0 \quad \text{and} \quad \varphi(S_0) = S_0.$$

Definition 2.7. *A vector field $\xi \in \theta_3$ is said to be tangent to $\widetilde{X}_0$ if and only if*

(1) $\xi(I(X_0)) \subseteq I(X_0)$,

(2) $\xi(I(S_0)) \subseteq I(S_0)$,

where $I(\cdot)$ denotes the defining ideal in $\mathcal{E}_3$.

Let $g = z - f^*(x,y)$. For a boundary b_s, we define the $\mathcal{E}_3$–module of logarithmic vector fields along the pair by

$$\mathfrak{X}_{\tan}(g, b_s) \;=\; \mathrm{Der}(-\log(g, b_s)) = \{\, \xi \in \theta_3 :\ \xi(g) \in \langle g \rangle,\ \ \xi(b_s) \in \langle g, b_s \rangle \,\}.$$

Remark 2.8. *If $\xi \in \mathfrak{X}_{\tan}(g, b_s)$, then it can be integrated to obtain a diffeomorphism germ $\varphi : (\mathbb{R}^3, 0) \to (\mathbb{R}^3, 0)$ that preserves $\widetilde{X}_0$.*

Definition 2.9. *We say that $h_1, h_2 \in \mathcal{E}_3$ are $\mathcal{R}(\widetilde{X}_0)$–equivalent if there exists a diffeomorphism germ $\varphi : (\mathbb{R}^3, 0) \to (\mathbb{R}^3, 0)$ that preserves $\widetilde{X}_0$ such that $h_2 = h_1 \circ \varphi$.*

Define

$$\Theta(\widetilde{X}_0) := \mathfrak{X}_{\tan}(g, b_s), \qquad \Theta^0(\widetilde{X}_0) = \{\xi \in \Theta(\widetilde{X}_0) : \xi(0) = 0\}.$$

Then, the tangent space and extended tangent space to the $\mathcal{R}(\widetilde{X}_0)$ orbit of h at h are

$$L\mathcal{R}(\widetilde{X}_0) \cdot h = \{\xi(h) : \xi \in \Theta^0(\widetilde{X}_0)\}, \qquad L_e\mathcal{R}(\widetilde{X}_0) \cdot h = \{\xi(h) : \xi \in \Theta(\widetilde{X}_0)\}.$$

On the other hand, the $\mathcal{R}_e^+$–codimension of h is

$$c(h) = \dim_{\mathbb{R}}\Big(\mathcal{M}_3 \,/\, L_e\mathcal{R}(\widetilde{X}_0) \cdot h\Big).$$

Now, set $f_x^* = \frac{\partial f^*}{\partial x}$, $f_y^* = \frac{\partial f^*}{\partial y}$, $b_x = \partial b_s/\partial x$, and $b_y = \partial b_s/\partial y$. Write $\partial_x, \partial_y, \partial_z$ for the coordinate vector fields on $\mathbb{R}^3$. We will use the following quasihomogeneous weights and weighted degree:

$$(w_x, w_y, d) = \begin{cases} (2, 1, 2), & \text{for} \quad b_1 = y^2 - x, \\ (1, 1, 2), & \text{for} \quad b_2 = y^2 - x^2, \\ (2, 3, 6), & \text{for} \quad b_3 = y^2 - x^3, \end{cases} \qquad \text{so that} \quad w_x x\, b_x + w_y y\, b_y = d\, b_s.$$

Consider the following five vector fields:

(1) $E = w_x x\, \partial_x + w_y y\, \partial_y + (w_x x\, f_x^* + w_y y\, f_y^*)\, \partial_z$ (Euler derivation).

(2) $L = b_y\, \partial_x - b_x\, \partial_y + (b_y f_x^* - b_x f_y^*)\, \partial_z$ (Koszul (tangential) derivation).

(3) $G_g = g\, \partial_z$ (Vertical g–multiple).

(4) $G_x = g\, \partial_x + (f_x^*\, g)\, \partial_z$ (g–multiples in x–directions).

(5) $G_y = g\, \partial_y + (f_y^*\, g)\, \partial_z$ (g–multiples in y–directions).

We have the following:

Lemma 2.10. *The $\mathcal{E}_3$–module $\mathfrak{X}_{\tan}(g, b_s)$ is generated by*

$$\{E,\ L,\ G_g,\ G_x,\ G_y\}.$$

Proof. The conditions for $\xi \in \theta_3$ to be tangent to $\widetilde{X}_0$ are

$$\exists\, \lambda, \mu, \nu \in \mathcal{E}_3 \ \text{ such that } \ \xi(g) = \lambda g, \qquad \xi(b_s) = \mu g + \nu b_s.$$

We have $g_x = -f_x^*$, $g_y = -f_y^*$, $g_z = 1$. So, these are precisely the syzygy conditions for the rows

$$(g_x, g_y, g_z, -g) \quad \text{and} \quad (b_x, b_y, 0, -g, -b_s).$$

A direct check shows that each of E, L, G_g, G_x, G_y satisfies the two conditions. Moreover, a Gröbner basis computation of syzygies in Singular shows that these five vector fields generate $\mathfrak{X}_{\tan}(g, b_s)$, in addition; it shows that they are minimal in all three boundary cases. □

Now, we classify submersion germs.

$$h : (\mathbb{R}^3, 0) \to (\mathbb{R}, 0)$$

up to $\mathcal{R}(\widetilde{X}_0)$–equivalence. To obtain this classification, we first recall several key concepts together with the relevant prenormal forms.

Definition 2.11. *[20] For $k \geq 1$ and $h \in \mathcal{E}_3$, define*

$$\mathrm{KS}_h^{(k)} :\ J^k\Theta(\widetilde{X}_0) \longrightarrow J^k\mathcal{M}_3, \qquad [\xi] \longmapsto j^k(\xi(h)).$$

We write $\mathrm{im}(\mathrm{KS}_h^{(1)})$ *and* $\mathrm{im}(\mathrm{KS}_h^{(2)})$ *for its linear and quadratic images.*

Remark 2.12. $\mathrm{KS}_h^{(k)}$ *is the Kodaira–Spencer map, and its action is restricted to jets.*

Proposition 2.13. *Let $h : (\mathbb{R}^3, 0) \to (\mathbb{R}, 0)$ be a submersion with $j^1h = \alpha x + \beta y + \gamma z$. Then*

$$\mathrm{im}(\mathrm{KS}_h^{(1)}) = \Big\langle\, j^1E(h),\ j^1L(h),\ j^1G_g(h),\ j^1G_x(h),\ j^1G_y(h)\,\Big\rangle = \langle\, w_x\alpha\, x + w_y\beta\, y, \Lambda_s, z\rangle,$$

where

$$\Lambda_s = j^1L(h) = \begin{cases} 2\alpha\, y + \gamma\, f_y^*, & b_1 = y^2 - x, \\ 2\beta\, x + 2\alpha\, y, & b_2 = y^2 - x^2, \\ 2\alpha\, y, & b_3 = y^2 - x^3. \end{cases}$$

In particular, $\langle z\rangle = \langle \alpha z, \beta z, \gamma z\rangle \subset \mathrm{im}(\mathrm{KS}_h^{(1)})$.

Proof. For $\xi = P\partial_x + Q\partial_y + R\partial_z$, we have

$$j^1(\xi(h)) = \alpha\, j^1P + \beta\, j^1Q + \gamma\, j^1R;$$

because $h_x(0) = \alpha$, $h_y(0) = \beta$, $h_z(0) = \gamma$, and the constants are killed in $J^1\mathcal{M}_3$. Now, we consider all vector fields.

For Euler field E, we have $j^1P = w_x x$, $j^1Q = w_y y$, and $j^1R = 0$ (the z–component is quadratic as f_x^*, f_y^* are linear). Therefore, we get

$$j^1E(h) = w_x\alpha\, x + w_y\beta\, y.$$

Next, for Koszul field L, we have $P = b_y$, $Q = -b_x$, $R = b_y f_x^* - b_x f_y^*$. Note that f_x^* and f_y^* are linear. So, $j^1(b_y f_x^*) = 0$ in all cases, while $j^1(-b_x f_y^*) = -b_x(0)\, f_y^*$. Thus,

$$j^1L(h) = \alpha\, j^1(b_y) + \beta\, j^1(-b_x) + \gamma\,(\, - b_x(0)\, f_y^*).$$

The evaluation of b_x, b_y yields the stated formulas for Λ_s:

$$b_1 = y^2 - x :\ j^1(b_y) = 2y,\ j^1(-b_x) = 1,\ -b_x(0) = 1\ \Rightarrow\ j^1L(h) = 2\alpha y + +\gamma f_y^*;$$
$$b_2 = y^2 - x^2 :\ j^1(b_y) = 2y,\ j^1(-b_x) = 2x,\ -b_x(0) = 0\ \Rightarrow\ j^1L(h) = 2\beta x + 2\alpha y;$$
$$b_3 = y^2 - x^3 :\ j^1(b_y) = 2y,\ j^1(-b_x) = 0,\ -b_x(0) = 0\ \Rightarrow\ j^1L(h) = 2\alpha y.$$

Finally, for G_g we have $P = Q = 0$, $R = g$. This implies that $j^1G_g(h) = \gamma\, j^1(g) = \gamma z$. On the other hand, for G_x and G_y, $P = g$, $Q = 0$, $R = f_x^* g$, and respectively $P = 0$, $Q = g$, $R = f_y^* g$. Because $j^1 g = z$ and $j^1(f^*_{(\cdot)} g) = 0$, we obtain

$$j^1G_x(h) = \alpha z, \qquad j^1G_y(h) = \beta z.$$

Therefore $\langle z\rangle = \langle \alpha z, \beta z, \gamma z\rangle$ is contained in the image. It follows that the displayed spanning set reduces to $\langle w_x\alpha x + w_y\beta y, \Lambda_s, z\rangle$. □

Remark 2.14. *For the boundary $b_1 = y^2 - x$, one has $b_x = -1$, $b_y = 2y$. So, the multiples of L by the coordinate functions contribute to linear terms. In particular,*

$$j^1((xL)(h)) = \beta\, x, \qquad j^1((yL)(h)) = \beta\, y.$$

Thus, for $s = 1$ the terms x and y can enter $\mathrm{im}(\mathrm{KS}_h^{(1)})$ via xL and yL (when $\beta \neq 0$).

Proposition 2.15. *Let $h : (\mathbb{R}^3, 0) \to (\mathbb{R}, 0)$ be a submersion with $j^1 h = \alpha x + \beta y + \gamma z$. Then, for every b_s and f^*, we have the unconditional inclusions*

$$\langle xz,\ yz,\ z^2\rangle \ \subset\ \mathrm{im}(\mathrm{KS}_h^{(2)}).$$

Moreover:

- *If $f^* = x^2 \pm y^2$, then $\langle x^2, xy, y^2\rangle \ \subset\ \mathrm{im}(\mathrm{KS}_h^{(2)})$. So, $\mathrm{im}(\mathrm{KS}_h^{(2)})$ contains all six quadratic monomials.*
- *If $f^* = x^2$, then $x^2, xy \in \mathrm{im}(\mathrm{KS}_h^{(2)})$. But, y^2 is missing at j^2 when $\alpha = \beta = 0$.*
- *If $f^* = y^2$, then $y^2, xy \in \mathrm{im}(\mathrm{KS}_h^{(2)})$. But, x^2 is missing at j^2 when $\alpha = \beta = 0$.*

Proof. First, note that at least one of α, β, γ is nonzero because h is a submersion. We have

$$j^1(G_g(h)) = \gamma z, \qquad j^1(G_x(h)) = \alpha z, \qquad j^1(G_y(h)) = \beta z.$$

If we multiply these vector fields by the linear functions x, y, z, then we obtain

$$xz,\ yz,\ z^2\ \in\ \mathrm{im}(\mathrm{KS}_h^{(2)}),$$

which proves the unconditional inclusions.

Next, to obtain the quadratic monomials in x, y, we use the Euler and Koszul generators. A direct jet computation gives

$$j^2(E(h)) = \gamma(w_x\, x\, f_x^* + w_y\, y\, f_y^*), \qquad j^2(L(h)) = \gamma(b_y\, f_x^* - b_x\, f_y^*).$$

Now, let $f^* = x^2 \pm y^2$. Then, $f_x^* = 2x$ and $f_y^* = \pm 2y$. Therefore,

$$j^2(E(h)) = \gamma(2w_x\, x^2 \pm 2w_y\, y^2).$$

So, whenever $\gamma \neq 0$, x^2 and y^2 lie in $\mathrm{im}(\mathrm{KS}_h^{(2)})$. On the other hand, if $\gamma = 0$ but α or β is nonzero, then $j^2(G_x(h)) = \alpha\, j^2(g) = \alpha\,(z - f^*)$ or $j^2(G_y(h)) = \beta\, j^2(g) = \beta\,(z - f^*)$ contribute $-\alpha f^*$ or $-\beta f^*$. Thus, we have again both x^2 and y^2 are obtained at order 2. For the mixed term, the 2-jet

$$j^2(L(h)) = \gamma(b_y\, f_x^* - b_x\, f_y^*)$$

contains the product $b_y \cdot f^*_x = 4xy$ and the $b_x f^*_y$. Note that the later part is at most linear or cubic in (x, y) (depending on the boundary type). Hence, it does not affect the j^2–term. Thus, we have $xy \in \mathrm{im}(\mathrm{KS}^{(2)}_h)$. Together, by $\langle x^2, xy, y^2\rangle \subset \mathrm{im}(\mathrm{KS}^{(2)}_h)$ and the first part, we obtain all six quadratic monomials.

Finally, let $f^* \in \{x^2, y^2\}$. Assume $f^* = x^2$ (the case $f^* = y^2$ is symmetric). Then $f^*_x = 2x$, $f^*_y = 0$. Hence, we have

$$j^2(E(h)) = \gamma\,(2w_x\, x^2), \qquad j^2(L(h)) = \gamma\,(b_y\, 2x),$$

whose quadratic truncations show that x^2 and xy belong to $\mathrm{im}(\mathrm{KS}^{(2)}_h)$. The monomial y^2 is absent at order 2 when $\alpha = \beta = 0$. Otherwise, the linear multiples of E or L by x or y provide the missing square. The case $f^* = y^2$ is identical to the interchanged cases x and y.

These computations establish all the stated inclusions. □

We recall the following standard notion.

Definition 2.16 (Finite determinacy [21, 22]). Let $h \in \mathcal{M}_3$, and let $G \subset Diff(\mathbb{R}^3, 0)$ act on $\mathcal{E}_3$ by the composition $h \mapsto h \circ \varphi$ for $\varphi \in G$. We say that h is *k–determined under G* if whenever $j^k h_1 = j^k h_2$, then we have that $h_1 \sim_G h_2$. If such a k exists, then h is said to be *finitely determined* under G.

Remark 2.17 (Mather's criterion [21, 22]). *If $\mathcal{M}_3^{k+1} \subset L_e G \cdot h$, then h is k–determined under G.*

In our setting, we only need the following jet consequence, which suffices for the codimension–≤ 2 classification.

Theorem 2.18. *Let $h : (\mathbb{R}^3, 0) \to (\mathbb{R}, 0)$ be a submersion on a model pair $\widetilde{X}_0$.*

(1) If $f^* = x^2 \pm y^2$, then $\mathrm{im}(\mathrm{KS}^{(2)}_h) = J^2\mathcal{M}_3$. In particular, $\mathcal{M}_3^3 \subset L_e\mathcal{R}(\widetilde{X}_0)\cdot h$, and h is 2–determined.

(2) If $f^* \in \{x^2, y^2\}$, then h is 2–determined except possibly in the special subcase when $j^1 h = z$. More precisely:

- *If $j^1 h \neq z$, then $\mathrm{im}(\mathrm{KS}^{(2)}_h) = J^2\mathcal{M}_3$. Hence, $\mathcal{M}_3^3 \subset L_e\mathcal{R}(\widetilde{X}_0)\cdot h$, and h is 2–determined.*
- *If $j^1 h = z$ and $f^* = x^2$ (resp. $f^* = y^2$), write $j^2 h = z + Ax^2 + Bxy + Cy^2$ (resp. $j^2 h = z + \tilde{A}y^2 + \tilde{B}xy + \tilde{C}x^2$). Then h is 2–determined if $C \neq 0$ when $f^* = x^2$, or $\tilde{C} \neq 0$ when $f^* = y^2$). If $C = 0$, then the inclusion $\mathcal{M}_3^3 \subset L_e\mathcal{R}(\widetilde{X}_0)\cdot h$ may fail at order 3.*

Proof. We first recall how the restricted Kodaira–Spencer map is related to the extended tangent space. By definition,

$$L_e\mathcal{R}(\widetilde{X}_0)\cdot h = \{\xi(h) : \ \xi \in \Theta(\widetilde{X}_0)\} \subset \mathcal{M}_3,$$

and the map

$$\mathrm{KS}^{(2)}_h : \ J^2\Theta(\widetilde{X}_0) \longrightarrow J^2\mathcal{M}_3, \qquad [\xi] \longmapsto j^2(\xi(h)),$$

has image

$$\mathrm{im}(\mathrm{KS}^{(2)}_h) = \{\, j^2(\xi(h)) : \ \xi \in \Theta(\widetilde{X}_0)\,\} = J^2(L_e\mathcal{R}(\widetilde{X}_0)\cdot h) \subset J^2\mathcal{M}_3.$$

Thus, whenever $\mathrm{im}(\mathrm{KS}^{(2)}_h) = J^2\mathcal{M}_3$, we have

$$J^2(L_e\mathcal{R}(\widetilde{X}_0)\cdot h) = J^2\mathcal{M}_3 = \mathcal{M}_3/\mathcal{M}_3^3.$$

Equivalently, the classes of elements of $L_e\mathcal{R}(\widetilde{X}_0)\cdot h$ generate the whole quotient $\mathcal{M}_3/\mathcal{M}_3^3$. If we set

$$Q \ := \ \mathcal{M}_3/L_e\mathcal{R}(\widetilde{X}_0)\cdot h,$$

then this is the statement that $Q/\mathcal{M}_3 Q = 0$, that is, $Q = \mathcal{M}_3 Q$. Because Q is a finitely generated $\mathcal{E}_3$–module, and $\mathcal{M}_3$ is the maximal ideal, Nakayama's lemma implies that $Q = 0$, so

$$\mathcal{M}_3 = L_e\mathcal{R}(\widetilde{X}_0)\cdot h.$$

In particular, $\mathcal{M}_3^3 \subset L_e\mathcal{R}(\widetilde{X}_0)\cdot h$, and Mather's criterion then gives that h is 2–determined. The case-by-case analysis below is precisely aimed at showing that $\mathrm{im}(\mathrm{KS}_h^{(2)}) = J^2\mathcal{M}_3$, except for the explicitly noted parabolic exception.

For $f^* \in \{x^2 \pm y^2\}$, Proposition 2.15 gives $\mathrm{im}(\mathrm{KS}_h^{(2)}) = J^2\mathcal{M}_3$. By Nakayama's lemma this implies that $\mathcal{M}_3^3 \subset L_e\mathcal{R}(\widetilde{X}_0)\cdot h$, hence 2–determinacy.

For $f^* \in \{x^2, y^2\}$, Proposition 2.15 yields the unconditional inclusions $\langle xz, yz, z^2\rangle \subset \mathrm{im}(\mathrm{KS}_h^{(2)})$. On the other hand, if $f^* = x^2$, then $x^2, xy \in \mathrm{im}(\mathrm{KS}_h^{(2)})$ (the same for $f^* = y^2$ by symmetry). If $j^1h \neq z$, then $j^1L(h)$ and $j^1E(h)$ provide linear terms. By multiplying these by suitable linear functions, we obtain the missing square at order 2 (e.g. for $f^* = x^2$, $j^1L(h) = 2\alpha y + \cdots$ and $j^2((yL)(h)) = 2\alpha\, y^2 + \cdots$, or $j^1E(h) = w_x\alpha x + w_y\beta y$ and $j^2((yE)(h)) = w_y\beta\, y^2 + \cdots$). Thus, $\mathrm{im}(\mathrm{KS}_h^{(2)}) = J^2\mathcal{M}_3$, which implies that it is 2–determinacy by Nakayama.

Now, assume $j^1h = z$ and take $f^* = x^2$ (the other case is symmetric). Then Proposition 2.15 shows that at order 2 the image contains $\{x^2, xy, xz, yz, z^2\}$. Because $\Theta(\widetilde{X}_0)$ is an $\mathcal{E}_3$–module, multiplying these quadratics by x, y, z produces all cubic monomials except possibly y^3. If the quadratic part of h has a nonzero y^2 term, say $j^2h = z + \cdots + Cy^2$ with $C \neq 0$, then $h_y = 2C\,y + \cdots$, and the Euler field E gives

$$j^3((yE)(h)) = y\cdot(w_y y\, h_y) + \cdots = 2w_y C\, y^3 + \cdots .$$

So, $y^3 \in J^3L_e\mathcal{R}(\widetilde{X}_0)\cdot h$. Together with the other cubic monomials obtained from x^2, xy, xz, yz, z^2, this yields $\mathcal{M}_3^3 \subset L_e\mathcal{R}(\widetilde{X}_0)\cdot h$ Hence, it is 2–determinacy. If $C = 0$, then no linear multiple of the generators produces y^3 at order 3. Therefore, $\mathcal{M}_3^3 \subset L_e\mathcal{R}(\widetilde{X}_0)\cdot h$ is not guaranteed, and Mather's sufficient criterion may fail in this subcase. □

We consider two codimensions for a submersion germ $h \in \mathcal{M}_3$ on a model pair $\widetilde{X}_0$. The *orbit codimension* is

$$c_{\mathrm{orb}}(h) \ = \ \dim_{\mathbb{R}}\Big(J^2\mathcal{M}_3/J^2L_e\mathcal{R}(\widetilde{X}_0)\cdot h\Big),$$

that is, the usual $\mathcal{R}_e^+$–codimension at the 2–jet level. When a normal form contains a *modulus a* (an intrinsic parameter not removable by $\mathcal{R}(\widetilde{X}_0)$–equivalence), we also record the *stratum codimension*

$$c_{\mathrm{str}}(h) \ = \ c_{\mathrm{orb}}(h) - 1.$$

If no modulus is present, we set $c_{\mathrm{str}}(h) = c_{\mathrm{orb}}(h)$. Note that; in our setting, the modality is at most 1.

In the *parabolic* case $f^* \in \{x^2, y^2\}$, let τ denote the coordinate *transverse* to f^*. So, for $f^* = x^2$, $\tau = y$, and for $f^* = y^2$, $\tau = x$. Thus the *transverse square* is simply τ^2.

Definition 2.19. *[27] An* unfolding *of h_0 with parameter space $(\mathbb{R}^c, 0)$ is a family*

$$H : (\mathbb{R}^3 \times \mathbb{R}^c, 0) \to (\mathbb{R}, 0), \qquad H(x; \lambda), \quad H(x; 0) = h_0(x).$$

We say H is versal *(with respect to G) if for every other unfolding $K(x, \mu)$ of h_0 there exists a change of parameter $\mu \mapsto \lambda(\mu)$ and a family of diffeomorphisms $\varphi_\mu \in G$ such that*

$$K(x, \mu) \;\equiv\; H(\varphi_\mu(x); \lambda(\mu)).$$

A versal unfolding is miniversal *if its parameter space has the minimal possible dimension.*

Proposition 2.20. *Let $h_0 \in \mathcal{E}_3$ and set*

$$Q \;=\; J^2\mathcal{M}_3 \,/\, J^2\!\big(L_e\mathcal{R}(\widetilde{X}_0) \cdot h_0\big).$$

If $m_1, \ldots, m_c \in J^2\mathcal{M}_3$ represent a basis of Q, then the family

$$H(x, y, z, \lambda) = h_0(x, y, z) + \sum_{i=1}^{c} \lambda_i m_i(x, y, z)$$

with parameters $\lambda = (\lambda_1, \ldots, \lambda_c)$, is a miniversal unfolding of h_0 for the $\mathcal{R}(\widetilde{X}_0)$–action.

Proof. This result is the relative analog of the standard construction in singularity theory. A miniversal unfolding of a germ is obtained by adding independent parameters along a basis of the quotient of the maximal ideal by the extended tangent space (truncated at the order of determinacy). In our setting, the same principle applies, with the tangent space taken relative to $\mathcal{R}(\widetilde{X}_0)$. □

We now classify submersion germs up to $\mathcal{R}(\widetilde{X}_0)$–equivalence with c_{str} at most 2.

Theorem 2.21. *Let $\widetilde{X}_0 = (X_0, S_0)$ be a model as above. If h is a submersion with $c_{\text{str}}(h) \leq 2$, then h is $\mathcal{R}(\widetilde{X}_0)$–equivalent to one of the normal forms listed in Tables 2 and 3.*

Table 2. Elliptic/hyperbolic point types $f^* \in \{x^2 \pm y^2\}$.

s	f^*	c_{orb}	c_{str}	submersion	miniversal unfolding
$s = 1$	$x^2 \pm y^2$	0	0	y	y
		0	0	x	x
		1	1	z	$z + \lambda x$
$s = 2$	$x^2 \pm y^2$	0	0	y	y
		0	0	x	x
		1	1	$x + y$	$x + y + \lambda (x - y)$
		1	1	$x - y$	$x - y + \lambda (x + y)$
		2	2	z	$z + \lambda_1 x + \lambda_2 y$
$s = 3$	$x^2 \pm y^2$	0	0	x	x
		1	1	y	$y + \lambda x$
		2	2	z	$z + \lambda_1 x + \lambda_2 y$

Table 3. Parabolic point types $f^* \in \{x^2, y^2\}$, Here, a is a modulus.

s	f^*	c_{orb}	c_{str}	submersion (normal form)	miniversal unfolding
$s=1$	$f^* = y^2$	0	0	y	y
		0	0	x	x
		2	2	z	$z + \lambda_1 x + \lambda_2 x^2$
$s=1$	$f^* = x^2$	0	0	y	y
		0	0	x	x
		3	2	$z + a\,\tau^2 \;\; (\tau = y)$	$z + \lambda_1 x + \lambda_2 y + a\,\tau^2$
$s=2$	$f^* = x^2$ or y^2	0	0	y	y
		0	0	x	x
		1	1	$x+y$	$x + y + \lambda\,(x-y)$
		1	1	$x-y$	$x - y + \lambda\,(x+y)$
		≥ 3	2	$z + a\,\tau^2$	$z + \lambda_1 x + \lambda_2 y + a\,\tau^2$
$s=3$	$f^* = x^2$ or y^2	0	0	x	x
		1	1	y	$y + \lambda\,x$
		≥ 3	2	$z + a\,\tau^2$	$z + \lambda_1 x + \lambda_2 y + a\,\tau^2$

Proof. We rely on the tangent module generators $\{E, L, G_g, G_x, G_y\}$ (Lemma 2.10), the 1–jet description (Proposition 2.13), and the 2–jet inclusions (Proposition 2.15. Together with the relative 2–determinacy result (Theorem 2.18), they provide the basic scheme for the classification.

More precisely, by Theorem 2.18, every submersion germ h with $c_{\text{str}}(h) \leq 2$ is $\mathcal{R}(\widetilde{X}_0)$–equivalent to a germ uniquely determined by its 2–jet. Thus, in order to obtain the normal forms in Tables 2–3, it is enough to classify the possible 2–jets $j^2 h$ up to the $\mathcal{R}(\widetilde{X}_0)$–action and to compute the corresponding orbit codimensions.

We begin with the linear classification, determined by $\text{im}(\text{KS}_h^{(1)})$. For a submersion h with $j^1 h = \alpha x + \beta y + \gamma z$, we have that

$$\text{im}(\text{KS}_h^{(1)}) = \langle\, w_x \alpha\, x + w_y \beta\, y,\ \Lambda_s,\ z \rangle,$$

where

$$\Lambda_s = \begin{cases} 2\alpha\, y + \gamma f_y^*, & b_1 = y^2 - x, \\ 2\beta\, x + 2\alpha\, y, & b_2 = y^2 - x^2, \\ 2\alpha\, y, & b_3 = y^2 - x^3. \end{cases}$$

For $s = 1$, the multiples xL, yL contribute $j^1((xL)(h)) = \beta x$, $j^1((yL)(h)) = \beta y$, while for $s = 2, 3$, these vanish at order 1.

Thus, the quotient $J^1\mathcal{M}_3/\text{im}(\text{KS}_h^{(1)})$ measures how many independent linear directions cannot be absorbed by the $\mathcal{R}(\widetilde{X}_0)$–action. Up to linear changes of coordinates preserving the model pair (X_0, S_0), these remaining linear directions can be chosen to be one of the basic forms

$$y, \quad x, \quad x \pm y, \quad \text{or} \quad z,$$

depending on which of α, β, γ vanish.

Concretely, we proceed case by case:

- For $s = 1$ (smooth edge), if $\beta \neq 0$, then Λ_1 already contains y, and the action generated by E and L allows us to eliminate any x–component. So the non-removable linear direction is represented by y, giving the normal form $h \sim y$. If $\beta = 0$, but $\alpha \neq 0$, then Λ_1 has no y–term, and the remaining nonzero direction can be chosen as x, hence $h \sim x$. If $\alpha = \beta = 0$, and $\gamma \neq 0$, then the only surviving linear direction is z, and we obtain $h \sim z$. These are exactly the three rows for $s = 1$ in Table 2.
- For $s = 2$ (corner), the two branch directions in the xy–plane are spanned by $u_\pm = (1, \pm 1)$, and $\Lambda_2 = 2\beta x + 2\alpha y$ controls the components in these directions. If both α and β are nonzero and not in the "diagonal" ratios, we can arrange, up to linear changes in (x, y) preserving $b_2 = y^2 - x^2$, that the nonremovable linear direction is simply x (or y), giving the first two rows for $s = 2$. If $\alpha = \beta \neq 0$ (respectively $\alpha = -\beta \neq 0$), then the remaining direction is along $x + y$ (respectively $x - y$), corresponding to the branchwise linear forms in the table. Finally, if $\alpha = \beta = 0$, and $\gamma \neq 0$, the only surviving linear direction is z, which yields the row with submersion z and $c_{\text{orb}} = 2$.
- For $s = 3$ (cusp), an analogous analysis of $\Lambda_3 = 2\alpha y$ shows that when $\alpha \neq 0$, we can take x as the distinguished linear form; when $\alpha = 0$, but $\beta \neq 0$, we obtain y up to $\mathcal{R}(\widetilde{X}_0)$–equivalence; and when $\alpha = \beta = 0$ (with $\gamma \neq 0$), we obtain z as the remaining direction. These are precisely the linear parts in the $s = 3$ rows of Tables 2 and 3.

This inspection of (α, β, γ) for each boundary type s produces the linear normal forms listed in the submersion column of both tables and determines their linear orbit codimensions.

Next, we consider the quadratic classification, which is governed by $\operatorname{im}(\mathrm{KS}_h^{(2)})$. Note that we always have $\langle xz, yz, z^2 \rangle \subset \operatorname{im}(\mathrm{KS}_h^{(2)})$. If $f^* = x^2 \pm y^2$, then all six quadratics lie in the image. If $f^* = x^2$ (resp. y^2), then x^2, xy (resp. y^2, xy) lie in the image, and the square τ^2 may be missing only when $\alpha = \beta = 0$ (i.e. $j^1 h = z$).

Thus, for each fixed boundary type s and point type f^*, the orbit codimension $c_{\text{orb}}(h)$ at the 2–jet level is exactly the number of independent linear directions missing from $\operatorname{im}(\mathrm{KS}_h^{(1)})$ plus, in the parabolic case with $j^1 h = z$, the possible additional missing quadratic direction τ^2. In particular, for $f^* = x^2 \pm y^2$, there are no quadratic moduli, while for $f^* \in \{x^2, y^2\}$, the only possible quadratic modulus comes from the class of τ^2.

In the elliptic/hyperbolic case $f^* = x^2 \pm y^2$, Proposition 2.15 shows that every quadratic monomial is in $\operatorname{im}(\mathrm{KS}_h^{(2)})$, so once the linear normal form has been fixed as above, no additional quadratic invariants remain. This gives exactly the entries in Table 2, and the values of c_{orb} and c_{str} there come solely from the missing linear directions.

In the parabolic case $f^* \in \{x^2, y^2\}$, the situation depends on whether $j^1 h$ is equal to z. When $j^1 h \neq z$, the linear forms described in Step 1 are present, and Proposition 2.15 together with the multiplication by x and y shows that even the transverse square τ^2 lies in the image of $\mathrm{KS}_h^{(2)}$. Hence, there is no quadratic modulus, and the normal forms are linear plus at most unfolding parameters, as in the first parabolic rows of Table 3.

Finally, we consider the appearance of the modulus a. The only genuinely new phenomenon occurs in the parabolic case when $j^1 h = z$, and $f^* \in \{x^2, y^2\}$. Then $\alpha = \beta = 0$, and Proposition 2.15 shows that at order 2 the image of $\mathrm{KS}_h^{(2)}$ contains all mixed and "vertical" quadratics x^2, xy, xz, yz, z^2, but the transverse square τ^2 is not in the image. Thus, the class of τ^2 in

$$J^2\mathcal{M}_3 \Big/ J^2 L_e \mathcal{R}(\widetilde{X}_0)\cdot h$$

is nonzero and one dimensional. Consequently, after fixing a linear normal form $j^1h = z$ and using the relative action to remove all other quadratic terms, we are left with a residual coefficient a of τ^2, so that the 2–jet takes the form

$$j^2h \sim z + a\,\tau^2.$$

This coefficient a cannot be killed by any $\mathcal{R}(\widetilde{X}_0)$–equivalence and therefore is a true modulus. Different values of a give inequivalent orbits, and this is exactly the phenomenon encoded by the entries with $z + a\,\tau^2$ in Table 3.

By Theorem 2.18, all entries with $f^* = x^2 \pm y^2$ are 2–determined. In the parabolic case, every entry listed with $c_{\mathrm{orb}} \leq 2$ is also 2–determined, and potential failures occur only when $j^1h = z$ and τ^2 is missing, which forces $c_{\mathrm{orb}} \geq 3$ and is therefore outside the theorem's hypothesis.

Therefore, for $c_{\mathrm{orb}}(h) \leq 2$, the classification reduces to 2–jets: $c_{\mathrm{orb}}(h)$ equals the number of missing linear directions in $\mathrm{im}(\mathrm{KS}_h^{(1)})$ plus, in parabolic $j^1h = z$ cases, the possible missing quadratic direction τ^2. We can easily check $s = 1, 2, 3$ and the point type f^* and obtain exactly the rows displayed in Tables 2 and 3. For the miniversal unfoldings, we add parameters along a basis of the corresponding quotient. When a modulus a occurs, it spans the missing τ^2 direction at order 2. So, fixing a reduces the codimension by 1, that is $c_{\mathrm{str}} = c_{\mathrm{orb}} - 1$, as indicated in the parabolic table. □

Remark 2.22. *When a modulus a appears in a displayed normal form (e.g. $z + a\,\tau^2$ in the parabolic case), the underlying reason is that the quadratic monomial τ^2 represents a genuinely new direction which is* not *generated by the restricted $\mathcal{R}(\widetilde{X}_0)$–action. More precisely, in the parabolic situation $f^* \in \{x^2, y^2\}$, the quadratic form has rank one, and τ denotes the coordinate transverse to its kernel. Proposition 2.15 shows that all mixed terms xy, as well as the "vertical" quadratics xz, yz, z^2, lie in the image of the restricted Kodaira–Spencer map, but the transverse square τ^2 does not. Consequently, the class of τ^2 in the quotient*

$$J^2\mathcal{M}_3 \,/\, J^2 L_e \mathcal{R}(\widetilde{X}_0)\cdot h$$

is nonzero, and no diffeomorphism preserving $\widetilde{X}_0$ can eliminate its coefficient.

Geometrically, the coefficient a measures the second–order behaviour of the height function in the transverse parabolic direction, and different values of a correspond to genuinely distinct $\mathcal{R}(\widetilde{X}_0)$–orbits. For this reason a is a true modulus rather than an unfolding parameter, and fixing its value removes exactly one independent quadratic direction, so the stratum codimension is

$c_{\mathrm{str}}(h) = c_{\mathrm{orb}}(h) - 1$. *In all other cases no such transverse square survives modulo the tangent space, and therefore no modulus appears.*

Example 2.23. Let $f^* = x^2 + y^2$, and consider the boundary type $s = 2$ with $b_2 = y^2 - x^2$. Thus, (X_0, S_0) is the corner model in the elliptic case. Define the submersion

$$h(x, y, z) = x + y + 2z + x^2 - 3xy + 5y^2 + xz - yz + z^2 + x^3.$$

Then

$$j^1h = x + y + 2z, \qquad j^2h = x + y + 2z + x^2 - 3xy + 5y^2 + xz - yz + z^2.$$

Because $f^* = x^2 + y^2$ is elliptic, Theorem 2.18 applies and shows that h is 2–determined under $\mathcal{R}(\widetilde{X}_0)$. In particular, the $\mathcal{R}(\widetilde{X}_0)$–equivalence class of h is completely determined by its 2–jet j^2h. On the other hand, higher order terms, such as the cubic term x^3, do not affect the classification.

Next, by Proposition 2.15, in the elliptic/hyperbolic case, we have

$$\mathrm{im}(\mathrm{KS}_h^{(2)}) = J^2\mathcal{M}_3 = \langle x^2, xy, y^2, xz, yz, z^2\rangle,$$

so each quadratic monomial lies in the image of the restricted Kodaira–Spencer map. Hence, the entire quadratic part

$$Q_2(x, y, z) = x^2 - 3xy + 5y^2 + xz - yz + z^2$$

belongs to $\mathrm{im}(\mathrm{KS}_h^{(2)})$. Therefore, there exists a vector field $\xi \in \Theta(\widetilde{X}_0)$ such that

$$j^2(\xi(h)) = Q_2.$$

Set $\tilde{h} := h - \xi(h)$. Then $\tilde{h}$ is $\mathcal{R}(\widetilde{X}_0)$–equivalent to h and satisfies

$$j^2\tilde{h} = x + y + 2z,$$

that is, all quadratic terms have been eliminated using the relative action.

We now simplify the linear part. For $s = 2$ and $j^1\tilde{h} = \alpha x + \beta y + \gamma z$ with $(\alpha, \beta, \gamma) = (1, 1, 2)$, Proposition 2.13 gives

$$\mathrm{im}(\mathrm{KS}_{\tilde{h}}^{(1)}) = \langle w_x\alpha x + w_y\beta y,\ \Lambda_2,\ z\rangle = \langle x + y,\ 2x + 2y,\ z\rangle = \langle x + y,\ z\rangle,$$

because $w_x = w_y = 1$ for $b_2 = y^2 - x^2$ and $\Lambda_2 = 2\beta x + 2\alpha y = 2x + 2y$. In particular, $z \in \mathrm{im}(\mathrm{KS}_{\tilde{h}}^{(1)})$, so we may modify $\tilde{h}$ by another element of $L_e\mathcal{R}(\widetilde{X}_0)\cdot \tilde{h}$ to adjust the coefficient of z in the 1–jet. Thus, there exists $\eta \in \Theta(\widetilde{X}_0)$ such that, for

$$h^{\mathrm{nf}} := \tilde{h} - \eta(\tilde{h}),$$

we have

$$j^1h^{\mathrm{nf}} = x + y.$$

Since quadratic terms have already been removed at the previous step and h is 2–determined, we obtain

$$j^2h^{\mathrm{nf}} = x + y.$$

We have therefore shown that h is $\mathcal{R}(\widetilde{X}_0)$–equivalent to the linear germ $x + y$, which appears as the codimension–1 normal form in Table 2 for the corner boundary ($s = 2$) in the elliptic case ($\alpha = \beta \neq 0$). This example illustrates how a submersion with nontrivial quadratic and cubic terms is reduced, via the restricted Kodaira–Spencer calculus and 2–determinacy, to the normal form $x + y$ listed in the classification.

Example 2.24. We now illustrate the parabolic case and the appearance of the modulus a in Table 3. Let $f^* = x^2$, and take boundary type $s = 1$; so that $\tau = y$ is the coordinate transverse to f^*. Thus, (X_0, S_0) is the edge model with parabolic point type $f^* = x^2$. Consider the submersion

$$h(x, y, z) = z + a\,y^2 + x^2 - 3xy + 2xz + z^2 + x^3 + y^3,$$

where $a \in \mathbb{R}$ is a fixed nonzero constant. Then

$$j^1 h = z, \qquad j^2 h = z + a\,y^2 + x^2 - 3xy + 2xz + z^2.$$

Because $j^1 h = z$, and $f^* = x^2$, this is precisely the exceptional parabolic situation in Theorem 2.18. We expand the 2–jet in the form

$$j^2 h = z + a\,y^2 + Q_2(x, y, z), \qquad Q_2 = x^2 - 3xy + 2xz + z^2,$$

so that the quadratic terms are separated into the transverse square y^2 and the remaining quadratic expression Q_2.

By Proposition 2.15, in the parabolic case $f^* = x^2$, we have

$$x^2,\ xy \in \mathrm{im}(\mathrm{KS}_h^{(2)}) \quad \text{and} \quad \langle xz, yz, z^2 \rangle \subset \mathrm{im}(\mathrm{KS}_h^{(2)}),$$

while y^2 is *not* in $\mathrm{im}(\mathrm{KS}_h^{(2)})$ when $j^1 h = z$ (i.e. when $\alpha = \beta = 0$ in the notation of Proposition 2.15). Hence, every quadratic monomial appearing in Q_2 lies in the image of the restricted Kodaira–Spencer map, and therefore $Q_2 \in \mathrm{im}(\mathrm{KS}_h^{(2)})$.

Consequently, Q_2 can be eliminated by an $\mathcal{R}(\widetilde{X}_0)$–change of coordinates preserving the model pair (X_0, S_0). More precisely, there exists a diffeomorphism germ φ preserving $\widetilde{X}_0$ such that

$$j^2(h \circ \varphi) = z + a\,y^2.$$

Denoting $\tilde{h} = h \circ \varphi$, we thus obtain

$$j^2 \tilde{h} = z + a\,y^2.$$

By Theorem 2.18, because the coefficient of y^2 is nonzero ($a \neq 0$), the germ h is 2–determined under the restricted $\mathcal{R}(\widetilde{X}_0)$ action. In particular, higher order terms such as $x^3 + y^3$ do not affect its $\mathcal{R}(\widetilde{X}_0)$–equivalence class, and we conclude that

$$h \ \sim_{\mathcal{R}(\widetilde{X}_0)} \ z + a\,y^2.$$

This is exactly the parabolic normal form $z + a\,\tau^2$ (with $\tau = y$) in Table 3 for $s = 1$, $f^* = x^2$, with $c_{\mathrm{orb}} = 3$ and $c_{\mathrm{str}} = 2$. The coefficient a cannot be removed by any $\mathcal{R}(\widetilde{X}_0)$–diffeomorphism, because y^2 lies outside $\mathrm{im}(\mathrm{KS}_h^{(2)})$. Note that different values of a give nonequivalent 2–jets and hence different $\mathcal{R}(\widetilde{X}_0)$–orbits. This explicitly realizes the role of a as a genuine modulus in the parabolic classification.

3. Height functions and contact classification

In the current section, we study the height functions on a regular surface in Monge form with a distinguished curve. Then, we classify the contact between height planes and the boundary at the origin.

Let $X \subset \mathbb{R}^3$ be given locally in Monge form

$$X = \{(x, y, z) \in \mathbb{R}^3 : \ z = f(x, y)\}, \qquad f(x, y) = \tfrac{1}{2}(k_1 x^2 + k_2 y^2) + a_{30}x^3 + a_{21}x^2 y + a_{12}xy^2 + a_{03}y^3 + \cdots$$

Here, k_1, k_2 are the principal curvatures at the origin along the x– and y–axes, respectively. We consider three model boundary types $S \subset X$ through the origin:

$$\begin{aligned} s = 1 \text{ (smooth edge)}: &\quad \gamma_1(t) = (t^2, t, f(t^2, t)), \\ s = 2 \text{ (corner)}: &\quad \gamma_{2,+}(t) = (t, t, f(t, t)), \qquad \gamma_{2,-}(t) = (t, -t, f(t, -t)), \\ s = 3 \text{ (cusp)}: &\quad \gamma_3(t) = (t^2, t^3, f(t^2, t^3)). \end{aligned}$$

Definition 3.1. *Let $v = (v_x, v_y, v_z) \in S^2$ be a unit vector, where S^2 is the 2-sphere. The ambient height function is*

$$h_v : (\mathbb{R}^3, 0) \to (\mathbb{R}, 0), \qquad h_v(x, y, z) = \langle (x, y, z), v \rangle = v_x x + v_y y + v_z z.$$

Its restriction to X is

$$H_v(x, y) = h_v(x, y, f(x, y)) = v_x x + v_y y + v_z f(x, y).$$

For $u \in X$, the height plane through u is the level set

$$\Pi(u, v) = \{w \in \mathbb{R}^3 : \langle w - u, v \rangle = 0\} = \{w \in \mathbb{R}^3 : h_v(w) = h_v(u)\}.$$

Given a boundary parameterization γ_s (with $s \in \{1, 2, 3\}$), boundary height germ *is*

$$\phi_v(t) = (h_v \circ \gamma_s)(t); \qquad \text{so that} \quad \phi_v(t) - \phi_v(0) = (H_v \circ \gamma_s)(t) - (H_v \circ \gamma_s)(0).$$

Remark 3.2. *(1) The plane $\Pi(u, v)$ depends only on the unoriented normal line $\{\pm v\}$ because $\Pi(u, v) = \Pi(u, -v)$ and $\phi_{-v} = -\phi_v$. Therefore, the A_k–type which is determined by $\phi_v - \phi_v(0)$ is independent of the choice of sign for v.*

(2) The germ $\phi_v - \phi_v(0)$ has A_k–type if and only if the first nonzero term in the Taylor expansion of $\phi_v(t)$ at $t = 0$ has order $k + 1$.

Definition 3.3. Let $u = \gamma_s(0) \in X$ and $v \in S^2$. The plane $\Pi(u, v) = \{h_v = h_v(u)\}$ has *A_k–contact* with X at u if the one variable germ $\phi_v(t) - \phi_v(0)$ is right–equivalent to t^{k+1}.

3.1. Contact along the boundary

We compute, for each boundary type $s = 1, 2, 3$, the first nonzero term of the boundary height germ

$$\phi_v(t) := (h_v \circ \gamma_s)(t), \qquad v = (v_x, v_y, v_z) \in S^2.$$

Then, we clasify the A_k class from the order of vanishing.

For $s = 1$, we have

$$\gamma_1(t) = (t^2, t, f(t^2, t)), \qquad f(t^2, t) = \tfrac{1}{2}k_2\, t^2 + a_{03}t^3 + \left(\tfrac{1}{2}k_1 + a_{12}\right)t^4 + a_{21}t^5 + a_{30}t^6 + \cdots,$$

so, for $v = (v_x, v_y, v_z)$,

$$\phi_v(t) = v_y\, t + \left(v_x + \tfrac{1}{2}k_2\, v_z\right)t^2 + (a_{03}v_z)t^3 + \left(\tfrac{1}{2}k_1 + a_{12}\right)v_z\, t^4 + \cdots. \tag{3.1}$$

Let c_m denote the coefficient of t^m in (3.1):

$$c_1 = v_y, \qquad c_2 = v_x + \tfrac{1}{2}k_2 v_z, \qquad c_3 = a_{03}v_z, \qquad c_4 = \left(\tfrac{1}{2}k_1 + a_{12}\right)v_z.$$

Right–classification gives A_{m-1} when the first nonzero term is t^m. Therefore, the contact type is A_{m-1}, where m is the least index with $c_m \neq 0$. Note that $v_y = 0$ means the plane contains the tangent $(0, 1, 0)$. If we add $v_x + \frac{1}{2}k_2 v_z = 0$, then v becomes proportional to the normal of the osculating plane at 0. Further, when a_{03} vanishes, then the contact is of order 4.

The above discussion is described explicitly in Table 4.

Table 4. Contact classification along γ_1.

Type	**Condition on** $v = (v_x, v_y, v_z)$	**Geometric meaning**
A_0	$v_y \neq 0$	Π transverse to boundary tangent $(0, 1, 0)$
A_1	$v_y = 0,\ v_x + \frac{1}{2}k_2 v_z \neq 0$	Π contains the tangent, not osculating
A_2	$v_y = 0,\ v_x + \frac{1}{2}k_2 v_z = 0,\ a_{03} v_z \neq 0$	Π equals the osculating plane
A_3	$v_y = 0,\ v_x + \frac{1}{2}k_2 v_z = 0,\ a_{03} = 0,\ (\frac{1}{2}k_1 + a_{12}) v_z \neq 0$	Quartic contact

Next, for $s = 2$, the boundary is the union of the two diagonal branches

$$\gamma_{2,+}(t) = (t, t, f(t, t)), \qquad \gamma_{2,-}(t) = (t, -t, f(t, -t)).$$

Along these, we have

$$f(t, t) = \tfrac{1}{2}(k_1 + k_2)t^2 + (a_{30} + a_{21} + a_{12} + a_{03})\, t^3 + \cdots,$$
$$f(t, -t) = \tfrac{1}{2}(k_1 + k_2)t^2 + (a_{30} - a_{21} + a_{12} - a_{03})\, t^3 + \cdots.$$

Hence,

$$\begin{aligned} \phi_v^{(+)}(t) &= (v_x + v_y)\, t + \tfrac{1}{2}(k_1 + k_2) v_z\, t^2 + (a_{30} + a_{21} + a_{12} + a_{03}) v_z\, t^3 + \cdots, \\ \phi_v^{(-)}(t) &= (v_x - v_y)\, t + \tfrac{1}{2}(k_1 + k_2) v_z\, t^2 + (a_{30} - a_{21} + a_{12} - a_{03}) v_z\, t^3 + \cdots. \end{aligned} \tag{3.2}$$

For each branch $\gamma_{2,\pm}$, the contact type at 0 is A_{m-1}, where m is the order of the first nonzero term of $\phi_v^{(\pm)}$ in (3.2). The two branches have tangents

$$\gamma'_{2,\pm}(0) = (1, \pm 1, 0), \qquad u_\pm = \tfrac{1}{\sqrt{2}}(1, \pm 1).$$

The linear term of the boundary height germs (3.2) is the orthogonality test with the branch tangents. Note that the linear coefficient of $\phi_v^{(\pm)}$ is

$$v_x \pm v_y = \langle (v_x, v_y),\ (1, \pm 1) \rangle.$$

Hence, $v_x \pm v_y = 0$ if and only if the height plane contains the corresponding tangent line.

Moreover, by Euler's formula, we have

$$k_n(u_\pm) = \tfrac{1}{2}\,(k_1 + k_2),$$

and the quadratic coefficient of (3.2) satisfies

$$\text{quadratic coefficient of } \phi_v^{(\pm)} = \tfrac{1}{2}\,(k_1 + k_2)\, v_z = k_n(u_\pm)\, v_z.$$

Therefore:

- A_0 occurs when $v_x \pm v_y \neq 0$ (plane transverse to the branch).

- A_1 occurs when $v_x \pm v_y = 0$, but $k_n(u_\pm)\, v_z \neq 0$ (plane contains the tangent and the normal curvature along the diagonal is nonzero).
- A_2 occurs when $v_x \pm v_y = 0$, and $k_n(u_\pm) = 0$ (i.e. $k_1 + k_2 = 0$), so the cubic term $(a_{30} \pm a_{21} + a_{12} \pm a_{03})v_z$ controls the contact on the corresponding diagonal.

The above discussion is summarized in Table 5.

Table 5. Corner ($s = 2$): contact classification along $\gamma_{2,+}$ and $\gamma_{2,-}$.

Branch	**Type**	**Condition on** v	**Geometric meaning**
$\gamma_{2,+}$	A_0	$v_x + v_y \neq 0$	Π transverse to tangent $(1, 1, 0)$
$\gamma_{2,+}$	A_1	$v_x + v_y = 0,\ (k_1 + k_2)v_z \neq 0$	Π contains the tangent; quadratic contact
$\gamma_{2,+}$	A_2	$v_x + v_y = 0,\ k_1 + k_2 = 0,$ $(a_{30} + a_{21} + a_{12} + a_{03})v_z \neq 0$	Cubic contact on $x = y$
$\gamma_{2,-}$	A_0	$v_x - v_y \neq 0$	Π transverse to tangent $(1, -1, 0)$
$\gamma_{2,-}$	A_1	$v_x - v_y = 0,\ (k_1 + k_2)v_z \neq 0$	Π contains the tangent; quadratic contact
$\gamma_{2,-}$	A_2	$v_x - v_y = 0,\ k_1 + k_2 = 0,$ $(a_{30} - a_{21} + a_{12} - a_{03})v_z \neq 0$	Cubic contact on $x = -y$

Finally, for $s = 3$, we have

$$\gamma_3(t) = (t^2, t^3, f(t^2, t^3)), \qquad f(t^2, t^3) = \tfrac{1}{2}k_1\, t^4 + \Big(\tfrac{1}{2}k_2 + a_{30}\Big)t^6 + a_{21}t^7 + a_{12}t^8 + a_{03}t^9 + \cdots,$$

so

$$\phi_v(t) = v_x\, t^2 + v_y\, t^3 + \tfrac{1}{2}k_1 v_z\, t^4 + \Big(\tfrac{1}{2}k_2 + a_{30}\Big)v_z\, t^6 + \cdots. \tag{3.3}$$

Let $c_2 = v_x$, $c_3 = v_y$, $c_4 = \frac{1}{2}k_1 v_z$, $c_6 = (\frac{1}{2}k_2 + a_{30})v_z$. Then, the contact type at 0 is A_{m-1}, where m are first indexed with $c_m \neq 0$; and described explicitly in Table 6.

Recall from Section 2 that

$$\kappa_{\text{sing}}(\gamma_3, 0) = \frac{3}{\sqrt{2}}, \qquad \tau_{\text{sing}}(\gamma_3, 0) = \sqrt{2}\, k_1,$$

with γ_3 of $(2, 3)$–type. Comparing these with the height expansion

$$\phi_v(t) = v_x\, t^2 + v_y\, t^3 + \tfrac{1}{2}k_1 v_z\, t^4 + \Big(\tfrac{1}{2}k_2 + a_{30}\Big)v_z\, t^6 + \cdots;$$

gives a direct link between the A_k–contact conditions and the singular invariants:

- A_2 occurs exactly when the height plane contains the cusp axis but it's not the tangent plane: $v_x = 0$, $v_y \neq 0$. This depends only on the *axis* (the tangent cone), not on κ_{sing} or τ_{sing}.
- A_3 occurs when the height plane equals the tangent plane $z = 0$, and the quartic term is nonzero: $v_x = v_y = 0$ and $k_1 v_z \neq 0$. Because $\tau_{\text{sing}} = \sqrt{2}\, k_1$, this is equivalent to $v_x = v_y = 0$ and $\tau_{\text{sing}}(\gamma_3, 0)\, v_z \neq 0$, that is, the quartic coefficient equals a fixed multiple of the singular torsion:

$$c_4 = \tfrac{1}{2}k_1 v_z = \frac{\tau_{\text{sing}}(\gamma_3, 0)}{2\sqrt{2}}\, v_z.$$

Thus A_3 is detected by τ_{sing}.

- A_5 is the axis–parabolic degeneracy: $v_x = v_y = 0$ and $k_1 = 0$, equivalently $\tau_{\text{sing}}(\gamma_3, 0) = 0$, while the next even term is nonzero:
$$c_6 = \left(\tfrac{1}{2}k_2 + a_{30}\right)v_z \neq 0.$$

In particular, the universal value $\kappa_{\text{sing}}(\gamma_3, 0) = 3/\sqrt{2}$ does not enter the dichotomy between A_3 and A_5. This means that split is governed by the singular torsion τ_{sing} via k_1. Moreover, $\kappa'_{\text{sing}}(\gamma_3, 0) = 0$ shows that, changes in viewing direction that keep the plane equal to $z = 0$ can affect the quartic contact through τ_{sing} alone.

The above discussion is summarized in Table 6.

Table 6. Contact classification along γ_3.

Type	**Conditions on** $v = (v_x, v_y, v_z)$	**Invariant form**	**Geometry**
A_1	$v_x \neq 0$	—	Π transverse to cusp axis $(1, 0, 0)$.
A_2	$v_x = 0$, $v_y \neq 0$	—	Π contains the axis; $\Pi \neq z = 0$.
A_3	$v_x = 0$, $v_y = 0$, $k_1 v_z \neq 0$	$c_4 = \dfrac{\tau_{\text{sing}}(\gamma_3, 0)}{2\sqrt{2}} v_z$	$\Pi = z = 0$; quartic contact governed by k_1 (equivalently by τ_{sing}).
A_5	$v_x = 0$, $v_y = 0$, $k_1 = 0$, $(\frac{1}{2}k_2 + a_{30})v_z \neq 0$	$\tau_{\text{sing}}(\gamma_3, 0) = 0$	Axis–parabolic degeneracy in $z = 0$; order-6 term controls contact.

3.2. Modeling height–plane contact by relative submersion normal forms

We now relate each height direction v to the $\mathcal{R}(\widetilde{X}_0)$–normal form of the ambient height function h_v, and then to the boundary contact from §3.1. Write

$$j^1 h_v = \alpha x + \beta y + \gamma z, \qquad (\alpha, \beta, \gamma) = (v_x, v_y, v_z).$$

The order of vanishing of the boundary height germ $\phi_v = h_v \circ \gamma_s$ computed in §3.1 determines the A_k–contact type. Moreover, it is compatible with the ambient reduction as follows,

$$h_v \sim_{\mathcal{R}(\widetilde{X}_0)} g \quad \Longrightarrow \quad h_v \circ \gamma_s \sim_{\mathcal{R}} g \circ \gamma_s,$$

that is, the restriction to the boundary has the same right–type. Indeed, if $g = h_v \circ \varphi$ with $\varphi \in Diff(\mathbb{R}^3, 0)$ preserving $\widetilde{X}_0$, then $g \circ \gamma_s = h_v \circ (\varphi \circ \gamma_s)$. On the other hand, because $\varphi \circ \gamma_s$ is a reparamatrization of the boundary branch, precomposition by γ_s sends ambient right–equivalences preserving $\widetilde{X}_0$ to right–equivalences of one–variable germs.

Note that h_v can have singularities of any c_{str} at points $u \in \widetilde{X}_0$ and for any $v \in S^2$; due to transversality constraints (see the Appendix in [26]).

Proposition 3.4. *Let $\widetilde{X}_0$ be a model of boundary type $s \in \{1, 2, 3\}$ and quadratic point type $f^* \in \{x^2 \pm y^2,\ x^2,\ y^2\}$. Then the $\mathcal{R}(\widetilde{X}_0)$–orbit of h_v is determined by $(\alpha, \beta, \gamma) = (v_x, v_y, v_z)$ as in Tables 7–9.*

Table 7. Elliptic/hyperbolic $f^* = x^2 \pm y^2$: ambient orbits and boundary contact.

Boundary	Condition on (α, β, γ)	Normal form	c_{str}	Boundary contact
$s = 1$	$\beta \neq 0$	y	0	A_0
	$\beta = 0,\ \alpha \neq 0$	x	0	A_1
	$\alpha = \beta = 0,\ \gamma \neq 0$	z	1	A_1
$s = 2$	$\alpha \neq \pm\beta$	x (or y)	0	$\gamma_{2,\pm}$: A_0 on both branches
	$\alpha = \beta \neq 0$	$x + y$	1	$\gamma_{2,+}$: A_0; $\gamma_{2,-}$: A_1 (elliptic), A_2 (hyperbolic)
	$\alpha = -\beta \neq 0$	$x - y$	1	$\gamma_{2,-}$: A_0; $\gamma_{2,+}$: A_1 (elliptic), A_2 (hyperbolic)
	$\alpha = \beta = 0,\ \gamma \neq 0$	z	2	$\gamma_{2,\pm}$: A_1 (elliptic), A_2 (hyperbolic)
$s = 3$	$\alpha \neq 0$	x	0	A_1
	$\alpha = 0,\ \beta \neq 0$	y	1	A_2
	$\alpha = \beta = 0,\ \gamma \neq 0$	z	2	A_3

Table 8. Parabolic $f^* = y^2$ (here $\tau = x$): ambient orbits and boundary contact.

Boundary	Condition on (α, β, γ)	Normal form	c_{str}	Boundary contact
$s = 1$	$\beta \neq 0$	y	0	A_0
	$\beta = 0,\ \alpha \neq 0$	x	0	A_1
	$\alpha = \beta = 0,\ \gamma \neq 0$	z	1	A_1
$s = 2$	$\alpha \neq \pm\beta$	x (or y)	0	$\gamma_{2,\pm}$: A_0 on both branches
	$\alpha = \pm\beta \neq 0$	$x \pm y$	1	As in Table 7.
	$\alpha = \beta = 0,\ \gamma \neq 0$	$z + a\tau^2$	2	$\gamma_{2,\pm}$: A_1 or A_2 as above
$s = 3$	$\alpha \neq 0$	x	0	A_1
	$\alpha = 0,\ \beta \neq 0$	y	1	A_2
	$\alpha = \beta = 0,\ \gamma \neq 0$	$z + a\tau^2$	2	A_3

Table 9. Parabolic $f^* = x^2$ (here $\tau = y$): ambient orbits and boundary contact.

Boundary	Condition on (α, β, γ)	Normal form	c_{str}	Boundary contact
$s = 1$	$\beta \neq 0$	y	0	A_0
	$\beta = 0,\ \alpha \neq 0$	x	0	A_1
	$\alpha = \beta = 0,\ \gamma \neq 0$	$z + a\tau^2$	2	A_2 (generic); A_3 if quartic
$s = 2$	$\alpha \neq \pm\beta$	x (or y)	0	$\gamma_{2,\pm}$: A_0 on both branches
	$\alpha = \pm\beta \neq 0$	$x \pm y$	1	$\gamma_{2,\pm}$: A_1 on the corresponding branch
	$\alpha = \beta = 0,\ \gamma \neq 0$	$z + a\tau^2$	2	$\gamma_{2,\pm}$: A_1 on both branches
$s = 3$	$\alpha \neq 0$	x	0	A_1
	$\alpha = 0,\ \beta \neq 0$	y	1	A_2
	$\alpha = \beta = 0,\ \gamma \neq 0$	$z + a\tau^2$	2	A_3

Finally, we relate the contact discriminants to the miniversal unfolding of the submersion normal form as follows.

Let $\Lambda = (\mathbb{R}^r, 0)$ be a parameter space, and let $F : (\mathbb{R}^3 \times \Lambda, 0) \to (\mathbb{R}, 0)$ be a deformation of a germ $g \in \mathcal{E}_3$ with $F(\cdot, 0) = g$. Write $H(u, \lambda) := F(u, \lambda)\big|_{u \in X_0}$. Choose a Monge chart $\Gamma : (\mathbb{R}^2, 0) \to (X_0, 0)$, $(x, y) \mapsto (x, y, f^*(x, y))$, and the standard boundary parameterizations $\gamma_1, \gamma_{2,\pm}, \gamma_3 \subset X_0$. Define

$$G(x, y, \lambda) := H(\Gamma(x, y), \lambda), \qquad \phi_{s,*}(t, \lambda) := H(\gamma_{s,*}(t), \lambda),$$

where $* \in \{\emptyset, +, -\}$ indexes the branch (for $s = 2$, $* = \pm$; for $s = 1, 3$, $* = \emptyset$).

Definition 3.5. *(1) The ambient height-discriminant is the critical value set*

$$\mathfrak{D}_X(F) := \{(\lambda, G(x, y, \lambda)) \in \Lambda \times \mathbb{R} : \ \partial_x G = \partial_y G = 0\}.$$

(2) For $m \geq 1$ and for each branch $\gamma_{s,*}$, set

$$\mathfrak{D}^{(m)}_{s,*}(F) := \{(\lambda, \phi_{s,*}(t, \lambda)) \in \Lambda \times \mathbb{R} : \ \partial_t \phi_{s,*} = \cdots = \partial_t^m \phi_{s,*} = 0\}.$$

Its projection

$$\Delta^{(m)}_{s,*}(F) := \pi_\Lambda(\mathfrak{D}^{(m)}_{s,*}(F)) \subset \Lambda$$

is the order–m contact discriminant locus for the branch $\gamma_{s,*}$.

Remark 3.6. Fix $s, *$. For generic $\lambda \notin \Delta^{(1)}_{s,*}(F)$, the contact is A_0 (resp. A_1 if $s = 3$). If $\lambda \in \Delta^{(1)}_{s,*}(F) \setminus \Delta^{(2)}_{s,*}(F)$, the contact is A_1. In general,

$$\lambda \in \Delta^{(m)}_{s,*}(F) \setminus \Delta^{(m+1)}_{s,*}(F) \iff \text{contact along } \gamma_{s,*} \text{ is } A_m.$$

Equivalently, the first nonzero derivative of $\phi_{s,*}(\cdot, \lambda)$ at the contact point has order $m+1$.

Proposition 3.7. *Let $F_1, F_2 : (\mathbb{R}^3 \times \Lambda, 0) \to (\mathbb{R}, 0)$ be deformations on $\widetilde{X}_0$. If F_1 and F_2 are P-$\mathcal{R}^+(\widetilde{X}_0)$–equivalent, then*

$$\mathfrak{D}^{(m)}_{s,*}(F_1) \ \cong \ \mathfrak{D}^{(m)}_{s,*}(F_2).$$

Consequently, their parameter projections $\Delta^{(m)}_{s,*}(F_i) = \pi_\Lambda(\mathfrak{D}^{(m)}_{s,*}(F_i)) \subset \Lambda$ are diffeomorphic. The same holds for the ambient discriminants $\mathfrak{D}_X(F_i)$.

Let $v = (v_x, v_y, v_z) \in S^2$, with $v_z = \gamma \neq 0$ and set

$$\lambda = \frac{v_x}{v_z}, \qquad (\lambda_1, \lambda_2) = \Big(\frac{v_x}{v_z}, \ \frac{v_y}{v_z}\Big).$$

At the 2-jet level (up to higher–order terms preserving $\widetilde{X}_0$),

$$s = 1 : \ \lambda = \alpha/\gamma, \qquad s = 2, 3 : \ (\lambda_1, \lambda_2) = (\alpha/\gamma, \beta/\gamma),$$

where $(\alpha, \beta, \gamma) = (v_x, v_y, v_z)$. Thus, linear contact discriminants in Λ pull back to linear conditions on v.

Recall that the miniversal families are

(1) $g = z + \lambda x$; and $g = z + \lambda_1 x + \lambda_2 y$; for $f^* = x^2 \pm y^2$ when $s = 1$ and $s = 2, 3$, respectively.

(2) $g = z + \lambda_1 x + \lambda_2 x^2$; for $f^* = y^2$; when $s = 1$.

(3) $g = z + \lambda_1 x + \lambda_2 y + a\,y^2$ (modulus a), for $f^* = x^2$, $s = 1$.

Proposition 3.8 (Linear order–1 contact discriminants)**.** *Assume $\gamma \neq 0$. and use $\lambda = \alpha/\gamma$ and $(\lambda_1, \lambda_2) = (\alpha/\gamma, \beta/\gamma)$ with $(\alpha, \beta, \gamma) = (v_x, v_y, v_z)$. Then the order–1 boundary–contact discriminant loci in the parameter space Λ are* linear *and are given in Table 10. Moreover, each row's linear subset of Λ pulls back under the normalization to the listed linear condition on the viewing direction v.*

Table 10. Combined contact data along γ_1, $\gamma_{2,\pm}$, and γ_3.

Curve	Case	Discriminant in Λ	Direction preimage (in v)
γ_1	Elliptic/Hyperbolic	$\{\lambda = -\frac{1}{2}k_2\}$	$\{ v_x + \frac{1}{2}k_2\, v_z = 0 \}$
γ_1	Parabolic ($f^* = y^2$)	$\{\lambda_1 = -\frac{1}{2}k_2\}$	$\{ v_x + \frac{1}{2}k_2\, v_z = 0 \}$
γ_1	Parabolic ($f^* = x^2$)	$\{\lambda_1 = 0\}$	$\{ v_x = 0 \}$
$\gamma_{2,+}$	Branchwise contact	$\{\lambda_1 + \lambda_2 = 0\}$	$\{ v_x + v_y = 0 \}$
$\gamma_{2,-}$	Branchwise contact	$\{\lambda_1 - \lambda_2 = 0\}$	$\{ v_x - v_y = 0 \}$
γ_3	Axis containment	$\{\lambda_1 = 0\}$ or $\{\lambda_2 = 0\}$	$\{ v_x = 0 \}$ or $\{ v_y = 0 \}$
γ_3	Tangent plane $\Pi = z = 0$	$\{\lambda_1 = \lambda_2 = 0\}$	$\{ v_x = v_y = 0 \}$

Remark 3.9. *The assumption $v_z = \gamma \neq 0$ is required so that the normalization $(\lambda_1, \lambda_2) = (\alpha/\gamma, \beta/\gamma)$ is well defined; when $v_z = 0$, the height parameterization in Monge form becomes degenerate.*

Let $\mathcal{D}_s \subset S^2$ be the direction discriminant, that is, the set of viewing directions for which the boundary contact order increases. Here, s corresponds to the boundary type. Then,

Corollary 3.10.

$$\begin{aligned}
\mathcal{D}_1 &= \{v_y = 0\} \cup \{v_y = 0,\ v_x + \tfrac{1}{2}k_2 v_z = 0\},\\
\mathcal{D}_2 &= \{v_x + v_y = 0\} \cup \{v_x - v_y = 0\} \cup \{v_x \pm v_y = 0,\ k_1 + k_2 = 0\},\\
\mathcal{D}_3 &= \{v_x = 0\} \cup \{v_x = v_y = 0\} \cup \{v_x = v_y = 0,\ k_1 = 0\}.
\end{aligned}$$

Remark 3.11. *(1) Each $\mathcal{D}_s$ is a semialgebraic subset of S^2 cut out by* linear *equations in v (with coefficients determined by the 2–jet of f). Under the normalization map $\Psi_s : v \mapsto (\lambda)$,*

$$\begin{aligned}
\Psi_1^{-1}\{\lambda = -\tfrac{1}{2}k_2\} &= \{v_x + \tfrac{1}{2}k_2 v_z = 0\},\\
\Psi_2^{-1}\{\lambda_1 \pm \lambda_2 = 0\} &= \{v_x \pm v_y = 0\},\\
\Psi_3^{-1}\{\lambda_i = 0\} &= \{v_i = 0\}.
\end{aligned}$$

Hence, $\mathcal{D}_s$ is the preimage of the parameter–space contact discriminant and inherits a natural, nested stratification by A_k–types.

(2) The defining equations of $\mathcal{D}_s$ have direct geometric meaning: $v_y = 0$ (resp. $v_x \pm v_y = 0$, $v_x = 0$) says that the height plane contains the boundary tangent (edge, diagonal, or cusp axis). The additional conditions $v_x + \frac{1}{2}k_2 v_z = 0$, $k_1 + k_2 = 0$, $k_1 = 0$ detect the next obstruction: osculating alignment for $s = 1$, vanishing diagonal normal curvature for $s = 2$, and vanishing singular torsion for $s = 3$. These are precisely the transitions from the linear normal forms to the z–strata in the miniversal families.

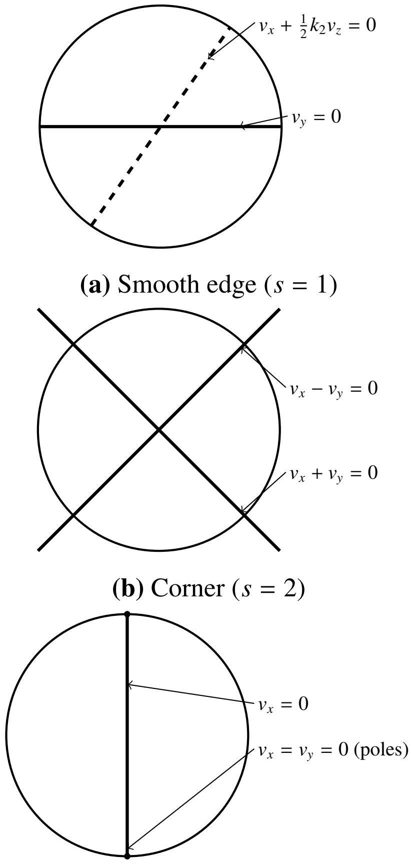

(a) Smooth edge ($s = 1$)

(b) Corner ($s = 2$)

(c) Cusp ($s = 3$)

Figure 2. Direction discriminants $\mathcal{D}_s \subset S^2$ for the three boundary types. Each disk provides a planar representation of the sphere of viewing directions, allowing the linear conditions governing increases in height–plane contact to appear as straight lines. In (a) (smooth edge, $s = 1$), the solid diameter identifies directions for which the height plane contains the edge tangent, while the dashed line marks the additional osculating alignment determined by the normal curvature. In (b) (corner, $s = 2$), the two diagonals correspond to the directions in which the height plane contains one of the two branch tangents. In (c) (cusp, $s = 3$), the vertical diameter represents the directions orthogonal to the cusp axis, and the poles $v_x = v_y = 0$ indicate the distinguished directions where the contact order increases. Taken together, these disks illustrate how specific loci in S^2 correspond to transitions in the type of height–plane contact along the boundary.

3.3. Applications and geometric meaning of the contact classification

The height function $h_v(w) = \langle w, v \rangle$ has a natural geometric interpretation in several settings. The A_k–classification of $h_v \circ \gamma_s$ on the distinguished boundary S can be used to describe how certain visible or physical features of (X, S) degenerate when the direction $v \in S^2$ varies. In particular, the direction discriminants $\mathcal{D}_s \subset S^2$ introduced in Section 3.1 consists of those directions v for which the order of contact between the height plane $\{h_v = h_v(0)\}$ and the boundary curve increases at the origin.

One convenient viewpoint is to regard v as a viewing direction. Then $h_v|_X$ is the orthogonal projection of X onto a plane perpendicular to v. The restriction $h_v \circ \gamma_s$ describes how the image of the boundary S appears in this projection. When the contact is of type A_0, the height plane intersects the boundary transversely, and the projected boundary is locally regular. If v crosses a component of $\mathcal{D}_s$, the contact type jumps to some A_k with $k \geq 1$. In that case, the projection of S develops a fold or a more complicated singular point (for example, a cusp in the silhouette). Thus, the sets $\mathcal{D}_s$ can be interpreted as bifurcation loci in the space of viewing directions. They mark exactly those directions for which the qualitative appearance of the boundary changes.

To illustrate this in a simple situation, consider the elliptic case $f(x, y) = \frac{1}{2}(x^2 + y^2)$ with a smooth boundary of type $s = 1$. In this case,

$$X = \{(x, y, z) : z = \tfrac{1}{2}(x^2 + y^2)\}, \qquad S = \gamma_1(t) = (t^2, t, f(t^2, t)).$$

For a unit vector $v = (v_x, v_y, v_z)$, the boundary height germ is

$$\phi_v(t) = (h_v \circ \gamma_1)(t) = v_y\, t + \left(v_x + \tfrac{1}{2}k_2 v_z\right)t^2 + a_{03} v_z t^3 + \cdots,$$

with $k_2 = 1$ at the origin in this model. If $v_y \neq 0$, then the first nonzero term is linear, so the contact is of type A_0, and the image of S in the projection along v is locally regular. Imposing $v_y = 0$ forces the height plane to contain the boundary tangent. The next coefficient, $v_x + \frac{1}{2}k_2 v_z$, determines whether the contact is A_1 or higher. If $v_y = 0$, but $v_x + \frac{1}{2}k_2 v_z \neq 0$, one obtains A_1–contact, corresponding to a simple tangency of the projected boundary. The additional condition $v_x + \frac{1}{2}k_2 v_z = 0$ produces an A_2–contact and a more degenerate point in the projection. In this way, the explicit equations from Section 3.1 can be read as concrete linear relations on (v_x, v_y, v_z). They describe how the silhouette of the edge changes as the viewpoint moves on S^2.

A second interpretation appears in mechanical models, where v is taken to be the direction of an external force or a supporting plane. The level sets $\{h_v = \text{const}\}$ form a family of planes orthogonal to v, and the order of contact with S measures how the surface can rest against such a plane. For a corner of type $s = 2$, the relations $v_x \pm v_y = 0$ characterize planes that contain the two branch tangents of S. The additional condition $k_1 + k_2 = 0$ (vanishing of the diagonal normal curvature) is responsible for the jump from A_1 to A_2 along each branch. In the cuspidal case $s = 3$, the conditions $v_x = 0$ and $v_x = v_y = 0$ describe planes containing the cusp axis or the tangent plane. The A_3/A_5 transition is governed by k_1 or, equivalently, by the singular torsion τ_{sing}. These relations show that the discriminants $\mathcal{D}_s$ encode, in a linear way, the special support directions for which the contact along an edge, corner or cusp becomes higher order. This is directly relevant to questions of balance and stability of rigid bodies with such boundary features.

A third family of examples arises in wavefront and optical models. If v is viewed as a propagation or illumination direction, the function h_v can be interpreted as a local phase function whose level sets approximate a moving front. Rays that graze the boundary S for directions v belonging to $\mathcal{D}_s$ have prolonged contact with the surface, and the A_k–type of $h_v \circ \gamma_s$ describes the resulting degeneracies in the associated caustic or focal set.

In the cuspidal case, for instance, the condition $v_x = v_y = 0$ corresponds to a front whose normal is orthogonal to both the cusp axis and the tangent plane. The singular torsion then decides whether the corresponding contact is of type A_3 or A_5. More generally, the linear conditions defining $\mathcal{D}_s$ in terms of (v_x, v_y, v_z) provide a simple and explicit way to track when the local interaction between a wavefront and an edge, corner or cusp changes its qualitative type. From this point of view, the relative classification obtained in this paper can be regarded as a local model for the behaviour of wavefronts near boundary singularities. The linear nature of the direction discriminants reflects the fact that these transitions are already encoded in the quadratic geometry of the surface and the boundary.

4. Conclusions

In this work, we studied regular surfaces $X \subset \mathbb{R}^3$ endowed with a distinguished boundary curve S of type $b_s = y^2 - x^s = 0$ for $s = 1, 2, 3$ (edge, corner, cusp), working under the restricted $\mathcal{R}(\widetilde{X})$-equivalence that preserves $\widetilde{X} = (X, S)$. We described explicitly the logarithmic module $\mathrm{Der}(-\log(g, b_s))$ (with $g = z - f^*(x, y)$), showing that it is generated by the five fields E, L, G_g, G_x, G_y. This yields a computable restricted Kodaira–Spencer calculus, a relative 2-determinacy theorem (with a single parabolic exceptional subcase), and an explicit classification of submersion germs of $\mathcal{R}(\widetilde{X})$-codimension ≤ 2.

We then applied this framework to height functions $h_v(w) = \langle w, v \rangle$. For each boundary type we obtained sharp A_k-contact criteria for the boundary height germs $h_v \circ \gamma_s$, expressed as linear conditions on the viewing direction $v \in S^2$. The resulting direction discriminants $\mathcal{D}_s \subset S^2$ are therefore linear in v and correspond, under the direction–parameter normalization, to linear discriminant strata in the relevant miniversal parameter spaces. In particular, in the cuspidal case the A_3/A_5 transition is governed by the singular torsion τ_{sing}.

Possible extensions include: (i) extending the relative determinacy and classification beyond codimension 2, where higher-order phenomena and additional moduli are expected; (ii) treating more general distinguished boundary singularities and configurations; and (iii) investigating further how the direction discriminants $\mathcal{D}_s$ relate to global bifurcation diagrams and caustic structures, arising in quasi(-border) equivalence settings.

Use of Generative-AI tools declaration

The author declares that he has not used Artificial Intelligence (AI) tools in the creation of this article.

Acknowledgments

The author would like to thank the editor and the anonymous reviewers for their helpful comments and suggestions.

Conflict of interest

The author declares no competing interest.

References

1. V. M. Zakalyukin, Quasi singularities, *Banach Center Publ.*, **82** (2008), 215–225.

2. V. M. Zakalyukin, Quasi-projections, *Proc. Steklov Inst. Math.*, **259** (2007), 273–280.
3. F. Alharbi, V. M. Zakalyukin, Quasi corner singularities, *Proc. Steklov Inst. Math.*, **270** (2010), 1–14. https://doi.org/10.1134/S0081543810030016
4. F. Alharbi, Quasi cusp singularities, *J. Singul.*, **12** (2015), 1–18. http://doi.org/10.5427/jsing.2015.12a
5. F. Alharbi, Bifurcation diagrams and caustics of simple quasi border singularities, *Topology Appl.*, **159** (2012), 38388. https://doi.org/10.1016/j.topol.2011.11.018
6. T. Tsukada, Genericity of caustics and wavefronts on an *r*-corner, *Asian J. Math.*, **14** (2010), 335–358. https://doi.org/10.4310/AJM.2010.v14.n3.a4
7. F. Alharbi, Vector fields on bifurcation diagrams of quasi singularities, *AIMS Math.*, **9** (2024), 1710–1736. https://doi.org/10.3934/math.20241710
8. F. Alharbi, R. Oset Sinha, Height functions on a cuspidal edge with a distinguished singular curve, *Port. Math.*, in press, 2025.
9. R. Oset Sinha, F. Tari, On the flat geometry of the cuspidal edge, *Osaka J. Math.*, **55** (2018), 393–421.
10. R. Oset Sinha, K. Saji, On the geometry of folded cuspidal edges, *Rev. Mat. Complut.*, **31** (2018), 627–650. https://doi.org/10.1007/s13163-018-0257-6
11. K. Teramoto, Cuspidal edges on focal surfaces of regular surfaces with parabolic points, preprint paper, 2025. https://doi.org/10.48550/arXiv.2509.00860
12. K. Saji, M. Umehara, K. Yamada, The geometry of fronts, *Ann. Math.*, **169** (2009), 491–529.
13. H. Terao, The bifurcation set and logarithmic vector fields, *Math. Ann.*, **263** (1983), 313–321. https://doi.org/10.1007/BF01457134
14. T. Abe, *Logarithmic Vector Fields and Freeness of Divisors and Arrangements*, Berlin: EMS Press, 2022.
15. F. Mofarreh, R. A. Abdel-Baky, Singularities of swept surfaces in Euclidean 3-space, *AIMS Math.*, **9** (2024), 26049–26064. https://doi.org/10.3934/math.20241272
16. A. A. Abdel-Salam, M. I. Elashiry, M. K. Saad, Tubular surface generated by a curve lying on a regular surface and its characterizations, *AIMS Math.*, **9** (2024), 12170–12187. https://doi.org/10.3934/math.2024594
17. M. Takahashi, H. Yu, On generalised framed surfaces in the Euclidean space, *AIMS Math.*, **9** (2024), 17716–17742. https://doi.org/10.3934/math.2024861
18. Y. Li, A. H. Alkhaldi, A. Ali, R. A. Abdel-Baky, M. K. Saad, Investigation of ruled surfaces and their singularities according to Blaschke frame in Euclidean 3-space, *AIMS Math.*, **8** (2023), 13875–13888. https://doi.org/10.3934/math.2023709
19. W. Zhang, P. Li, D. Pei, Circular evolutes and involutes of spacelike framed curves and their duality relations in Minkowski 3-space, *AIMS Math.*, **9** (2024), 5688–5707. https://doi.org/10.3934/math.2024276
20. K. Kodaira, D. C. Spencer, On deformations of complex analytic structures I, II, *Ann. Math.*, **67** (1958), 328–466.

21. J. N. Mather, Stability of C^∞ mappings. VI. The nice dimensions, *Proc. Sympos. Pure Math.*, **27** (1975), 207–253.

22. J. Montaldi, *Singularities, Bifurcations and Catastrophes*, Cambridge: Cambridge University Press, 2021.

23. V. I. Arnol'd, S. M. Gusein-Zade, A. N. Varchenko, *Singularities of Differentiable Maps I*, Boston: Birkhäuser, 1985.

24. V. I. Arnol'd, *Singularities of Caustics and Wave Fronts*, Dordrecht: Kluwer Academic, 1990.

25. J. W. Bruce, P. J. Giblin, *Curves and Singularities: A Geometrical Introduction to Singularity Theory*, 2 Eds., Cambridge: Cambridge University Press, 1984.

26. J. W. Bruce, J. M. West, Functions on a manifold with boundary, *Topology*, **37** (1998), 613–623.

27. V. I. Arnol'd, *Singularities of Caustics and Wave Fronts*, Dordrecht: Kluwer Academic, 1990.